CREWES

Research Report 2021
Volume 33

In this volume…

Report Summaries

*For **Complete Reports** and **Student Theses** please visit:*

https://www.crewes.org

(Sign in/password required)

UNIVERSITY OF CALGARY
FACULTY OF SCIENCE
Department of Geoscience

Notice of Intent to Publish

Please note that the authors of the research in this 33rd Volume of the Abstract Book intend to publish or otherwise publically disseminate their full research papers in the coming calendar year. According to the contracts between the University of Calgary (CREWES) and each Sponsor, the University will make available to the Sponsor a copy of the proposed publication resulting from the CREWES Project prior to submission for publication. In the event that the Sponsor determines that Research Results within the proposed publication contain Sponsor Confidential Information, the Sponsor shall have thirty (30) days to notify the University in writing and the University shall remove Sponsor Confidential information prior to publication. This 30 day period shall be considered to have started at the end of this meeting (December 3, 2021). These full research reports are available on the CREWES website to all Sponsors and their employees.

In memory of Bernie Law

This year CREWES lost a family member. We are mourning the passing of Bernie Law.

Bernie was fighting cancer for the last three years. He came to our group in 2016 after a long and successful career as a developer in the Calgary geophysical community. Bernie wanted to finish his working and intellectual journey by achieving a Ph.D. In spite of the hardships he had to suffer, he achieved his goal. Although his health did not allow him to go through the final Ph.D. defence, the university granted him his Ph.D. and on his last day, he was able to savour his victory.

Bernie was an example of dedication and enthusiasm. His only flaw was he could not stop widening his research. Although he wanted to try every new idea, he was able to finish writing his thesis about traveltime tomography just in time. His work includes leading-edge topics like stereo-tomography, two published papers and several conference presentations. His last paper, now published in the Canadian Journal of Seismic Exploration, contains his last flashes of creative energy and enthusiasm.

In CREWES we will miss Bernie enormously. He was a friend to all, always helping in every possible way, sharing his knowledge, experience and most of all, his happiness of being a student again. Bernie, farewell, you will be with CREWES always.

Daniel Trad

CREWES in 2021

It is again my privilege and pleasant responsibility to welcome you to the 2021 CREWES Annual Sponsors' Meeting and technical review. Like last year, 2021 has been a year where the global pandemic has been a dominant feature. Although we are all very hopeful that we are moving out of the worst of it, it has been another year of uncertainty for us, personally and professionally. My thoughts and good wishes go out to your families, friends, and close colleagues for their continued health and safety.

We developed an approach to making progress and continuing what I believe is our ground-breaking research in 2021. Made up of slightly reduced and highly regulated lab and field work, online meetings, planning sessions, and remote research. I want to give a big shout-out to all CREWES researchers who have produced the results we are presenting this year under this strange – and quite isolating – experience.

We lost a good friend and colleague this year, Bernie Law. He was a Ph.D. student who had been working with Daniel Trad for several years, but who was also well known to the Calgary and international geophysics community after a long and productive career in industry. An effort spearheaded by Daniel and supported across the University led to Bernie being awarded his Ph.D. despite the challenges resulting from his health, which made a conventional final evaluation impossible. Daniel will speak about Bernie and his legacy at our meeting.

The year has had some fantastic highlights. In-house elastic full waveform inversion codes have been applied to our 2018 "Snowflake" DAS and accelerometer VSP dataset, which was acquired in collaboration with the Containment and Monitoring Institute (CaMI), with fascinating and encouraging results moving us towards reservoir FWI in monitoring. Our CREWES Data Science Initiative and machine learning methods are pushing into new areas of AI, producing new definitions of waveform inversion and procedures for learning the elastic wave equation. Our ability to acquire DAS data has taken a leap forward as well: in 2021 we participated with a group of researchers to acquire a DAS interrogator unit, and our main 2021 field campaign took that IU out for a spin. We have also continued to push application of our seismic research into high-impact application areas such as geothermal and CO_2.

CREWES relies on the financial support of our sponsors. We realize all too well how much work is needed on the part of our sponsor representatives and supporters to initiate and maintain that kind of support. Please let me conclude with a big thank-you on behalf of the CREWES team. We look forward to continuing to make your effort and support worthwhile over the coming years.

Calgary, Alberta
December, 2021

Kristopher Innanen
CREWES Director

Table of Contents

* Video Presenter

2021 CREWES Sponsors

Acceleware	Aramco Services Company
CGG	Chevron Corporation
Devon Energy Corporation	INOVA Geophysical
Japan Oil, Gas and Metals National Corporation	Petrobras
Petronas Carigali SDN BHD	TGS

Natural Sciences and Engineering Research Council of Canada (NSERC) - Collaborative Research and Development Grant

NSERC CRSNG

Additional funding provided by:

CANADA FIRST RESEARCH EXCELLENCE FUND

CREWES Personnel 2021

LEADERSHIP

Kristopher A. Innanen, Director
Professor, Department of Geoscience, University of Calgary

B.Sc. Physics and Earth Science, 1996, York University
M.Sc. Physics, 1998, York University
Ph.D. Geophysics, 2003, University of British Columbia

- Work Experience: University of Houston

Don C. Lawton, Associate Director
Director for Containment and Monitoring Institute (CaMI)

Faculty Professor, Department of Geoscience, University of Calgary

B.Sc. (Hons. Class I) Geology, 1973, University of Auckland
Ph.D. Geophysics, 1979, University of Auckland

- Work Experience: New Zealand Steel Mining Ltd., Amoco Minerals (N.Z.) Ltd., Carbon Management Canada

Daniel Trad, Associate Director
Associate Professor, Department of Geoscience, University of Calgary

Licenciatura in Geophysics, 1994, Universidad Nacional de San Juan, Argentina
Ph.D Geophysics, 2001, University of British Columbia

- Work Experience: Electromagnetic Methods (Argentina and Brazil), Seismic Research and development (Veritas, CGG, Techco, in Calgary and France)

Michael P. Lamoureux
Faculty Professor, Department of Mathematics and Statistics, University of Calgary

B.Sc. Mathematics, 1982, University of Alberta
M.Sc. Mathematics, 1983, Stanford University
Ph.D. Mathematics, 1988, University of California, Berkeley

- Work Experience: Farallon Computing, NSERC Canada, FuseForward

Kevin W. Hall, Technical Manager

B.Sc. Geophysics, 1992, University of Calgary
M.Sc. Geophysics, 1996, University of Calgary

- Work Experience: Lithoprobe Seismic Processing Facility at the University of Calgary

RESEARCH STAFF, POST DOCS AND VISITING SCHOLARS

Kevin L. Bertram

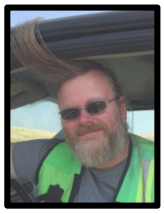

Electronics Technician Certificate, 2005, Southern Alberta Institute of Technology

- Work Experience: Aram Systems Ltd.

Malcolm B. Bertram

B.Sc. Geology, Auckland, New Zealand

- Work Experience: GSI (Western Australia), Western Geophysics (Western Australia), Auckland University, University of Calgary

Xiaohui Cai

B.Sc. Geophysics, 2011, Yangtze University, Hubei, China
Ph.D. Geophysics, 2016, China University of Petroleum

- Work Experience: Nanjing Tech University, The University of Texas at Austin

Marcelo Guarido de Andrade

B.Sc. Physics, 2006, University of São Paulo, Brazil
M.Sc. Geophysics, 2008, University of São Paulo, Brazil
Ph.D. Geophysics, 2017, University of Calgary

- Work Experience: Verdazo Analytics, Schlumberger (Houston), PGS (Rio de Janeiro, Brazil), Orthogonal Geophysics, Husky Energy

David C. Henley

B.Sc. Physics, 1967, Colorado State University
M.Sc. Physics, 1968, University of Michigan

- Work Experience: Shell Oil Co., Shell Canada Ltd.

Helen Isaac

B.Sc. Mathematics, 1973, Imperial College, London
M.Sc. Geophysics, 1974, Imperial College, London
Ph.D. Geophysics, 1996, University of Calgary

- Work Experience: Phillips Petroleum Company, Hudson's Bay Oil and Gas, Canterra Energy, Husky, Fold-Fault Research Project at the University of Calgary

Scott Keating

B.Sc. with Honours in Physics 2014, University of Alberta
Ph.D. Geophysics, 2020, University of Calgary

- Work Experience: CNOOC International

Marie Macquet

B.Sc. Earth Science, 2009, University of Nantes (France)
M.Sc. Planetology, 2011, University of Nantes (France)
Ph.D. Geophysics, 2014, Isterre, University of Grenoble (France)

Shahpoor Moradi

B.Sc. Applied Physics, 2000, University of Razi, Iran
M.Sc. Theoretical Physics, 2002, University of Razi, Iran
Ph.D. Theoretical Physics, 2006, University of Razi, Iran
Ph.D. Geophysics, 2017, University of Calgary)

Yichuan Wang

B.Eng. Geological Engineering, 2013, China University of Mining and Technology, Beijing, China
Ph.D. Geophysics, 2019, University of Saskatchewan

- Work Experience: Joanneum Research, The University of Oklahoma

Joe Wong

B.Sc. Physics/Mathematics, 1971, Queen's University
M.Sc. Applied Geophysics, 1973, University of Toronto
Ph.D. Applied Geophysics, 1979, University of Toronto
Work Experience: Ontario Ministry of the Environment, University of Toronto, JODEX Applied Geoscience Limited, CREWES

GRADUATE STUDENTS

Ninoska Amundaray

B.Sc. Geophysical Engineering, 2016, Simon Bolivar University, Venezuela

- Work experience: PDVSA, Venezuela

Farzaneh Bayati

B.Sc. Physics, 2008, University of Science and Technology
M.Sc. Geophysics Exploration, 2012, University of Tehran

- Work experience: Tehran Energy Consultants company (TEC), Tehran, Iran

Matt Eaid

B.Sc. (First Class Honours) Geophysics, 2015, University of Calgary

- Work experience: Shell Canada Ltd., Husky Energy, Chevron Energy Technology Company

David Emery

M.Sc. Geophysics, 2006, University of Calgary

- Work experience: Husky Energy

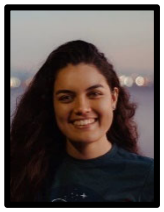

Paloma Lira Fontes

B.Sc. Geophysics, 2018, Federal University of Bahia

Xin Fu

B.Sc. Geophysics, 2015, China University of Petroleum (East China)
M.Sc. Geophysics, 2018, China University of Petroleum(Beijing)

Scott Hess

M.Sc. Geophysics, 2006, Boise State University

- Work Experience: Equinor

Qi Hu

B.Sc. Geophysics, 2011, Yangtze University, Hubei, China
M.Sc. Geophysics, 2014, China University of Petroleum, China

- Work Experience: Sinopec Geophysical Research Institute

Shang Huang

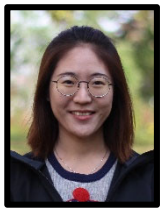

B.Eng. Geophysics, 2017, China University of Petroleum, China
M.Sc. Geophysics, 2018, University of Calgary

Brendan Kolkman-Quinn

B.Sc. with Honours in Physics, 2009, University of Alberta
B.Sc. Geophysics, 2014, University of Calgary

- Work Experience: ConocoPhillips Canada

Da Li

B.Sc. Geophysics, 2012, China University of Geosciences (Beijing)
M.Sc. Geophysics, 2016, China University of Geosciences (Beijing)

Jinji Li

B.Sc. Exploration Geophysics, 2017, Ocean University of China
M.Sc. Geophysics, 2020, Tongji University

- Work Experience: The First Institute of Oceanography of China, DTCC

Ellen Liu

B.Sc. Chemical Engineering, 2014, University of Alberta

- Work Experience: ConocoPhillips Canada

He Liu

B.Sc. Prospecting Technology and Engineering, 2012, China University of Petroleum (Beijing)
M.Sc. Geophysics, 2014, China University of Petroleum (Beijing)
Ph.D. Geophysics, 2019, China University of Petroleum (Beijing)

Mariana Lume

B.Sc. Geophysical Engineering, 2019, Simon Bolivar University
- Work Experience: PDVSA Intevep

Jorge Monsegny

B.Sc. Computer Science, 2003, National University of Colombia
M.Sc. Mathematics, 2007, National University of Colombia
- Work Experience: Santander Industrial University, Ecopetrol ICP, National University of Colombia

Luping Qu

B.Sc. Geophysics, 2014, China University of Petroleum (East China)
M.Sc. Geophysics, 2017, China University of Petroleum (Beijing)

Lukas Sadownyk

B.Sc. with honours Geophysics, 2020, University of Calgary
B.Sc. with distinction Geology, 2020, University of Calgary
- Work Experience: Valeura Energy, Gran Tierra, Imperial Oil, CNRL

Ziguang Su

B.Eng. Exploration Geophysics, 2017, China University of Petroleum, China
B.A. English, 2017, China University of Petroleum
M.Sc. Geophysics, 2018, University of Calgary

Tianze Zhang

B.Sc. Applied Geophysics, 2015, Jilin University, China
M.Sc. Geological Engineering, 2018, Jilin University, China

Kai Zhuang

B.Sc. Geophysics, 2018, University of Calgary

ASSOCIATED FACULTY and SCIENTISTS

Huaizhen Chen
Research Fellow, Tongji University, Shanghai, China
Adjunct Researcher, CREWES, University of Calgary
Ph.D. Geophysics, 2015, China University of Petroleum
B.Sc. Geophysics, 2010, China University of Petroleum

Andreas Cordsen
Technical Advisor, CREWES, University of Calgary
M.Sc. Geology, 1975, Queen's University, Kingston
M.Sc. Geophysics, 1980, Dalhousie University, Halifax
- Work Experience: BEB, Esso Resources, Norcen Energy, GEDCO, Schlumberger, CHAD Data Ltd.
-

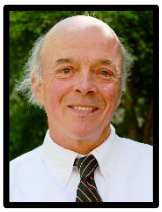

Sam Gray
Technical Advisor, CREWES, University of Calgary
B.S. Math, 1970, Georgetown University
Ph.D. Math, 1978, University of Denver
- Work experience: U.S. Naval Research Lab, General Motors Institute, Amoco, BP, Veritas, CGG

Rachel Lauer
Assistant Professor, University of Calgary
B.Sc. Psychology, Bryn Mawr College
M.Sc. Environmental Engineering Geoscience, Radford University
Ph.D. Geoscience, Pennsylvania State University
- Work Experience: Consultant at NAEVA Geophysics

Faranak Mahmoudian
Technical Advisor, CREWES, University of Calgary
B.Sc. Applied Physics, 2000, K. N. Toosi University of Technology, Iran
M.Sc. Geophysics, 2006, University of Calgary
Ph.D. Geophysics, 2013, University of Calgary
- Work Experience: Shell Canada, Earth Signal Processing

Gary F. Margrave, Emeritus Director
Emeritus Professor, Faculty Professor, Department of Geoscience, University of Calgary

B.Sc. Physics, 1975, University of Utah
M.Sc. Physics, 1977, University of Utah
Ph.D. Geophysics, 1981, University of Alberta

- Work Experience: Chevron Canada Resources, Chevron Geoscience Company, Devon Canada, TGS Canada

Brian H. Russell
Adjunct Professor, Department of Geoscience, University of Calgary

B.Sc. Physics, 1972, University of Saskatchewan
Honours Certificate in Geophysics, 1975, University of Saskatchewan
M.Sc. Geophysics, 1978, University of Durham
Ph.D. Geophysics, 2004, University of Calgary

- Work Experience: Chevron Geoscience Company, Teknica Resource Development, Veritas Software Ltd., Hampson-Russell Software Ltd, CGG GeoSoftware

Roman Shor
Assistant Professor, Department of Chemical and Petroleum Engineering, University of Calgary

Associate Head (Undergraduate Studies), Department of Chemical and Petroleum Engineering, University of Calgary

B.Sc. Computer Science, 2009, University of Pennsylvania
M.Sc. Computer Science, 2010, University of Pennsylvania
M.Sc. Petroleum Engineering, 2014, University of Texas at Austin
Ph.D. Petroleum Engineering, 2016, University of Texas at Austin

- Work Experience: Shell, Merck, Lehman Brothers

Robert R. Stewart
Cullen Chair in Exploration Geophysics, University of Houston

Adjunct Professor, Department of Geoscience, University of Calgary

B.Sc. Physics and Mathematics, 1978, University of Toronto
Ph.D. Geophysics, 1983, Massachusetts Institute of Technology

- Work Experience: Veritas Software Ltd., Gennix Technology Corp., University of Calgary

Xiucheng Wei
Technical Advisor, CREWES, University of Calgary

B.Sc. Geophysics, 1982, China University of Petroleum
M.Sc. Geophysics, 1992, China University of Petroleum
Ph.D. Geophysics, 1995, China University of Petroleum

- Work Experience: China National Petroleum Company (CNPC), China University of Petroleum (CUP), British Geological Survey (BGS), China Petroleum & Chemical Corporation (Sinopec), International Research Coordinator with the Faculty of Science at the University of Calgary

Matt Yedlin
Associate Professor, Department of Electrical and Computer Engineering, University of British Columbia

B.Sc. Honours Physics, 1971, University of Alberta
M.Sc. Physiology, 1973, University of Toronto
Ph.D. Geophysics, 1978, University of British Columbia

- Work Experience: Conoco

Student Theses

The following theses were completed with CREWES in 2021:

M.Sc.	Farzaneh Bayati	3-D data Interpolation and denoising by adaptive weighting rank-reduction method usingsingular spectrum analysis algorithm
Ph.D.	Mathew Vernon Eaid	Distributed acoustic sensin: modelling, full waveform inversion, and its use in seismic monitoring
Ph.D.	Bernie Ki-Yun Law	Traveltime tomography for land seismic data
Ph.D	Da Li	Novel Optimization Schemes for Full waveform Inversion: Optimal Transport and Inexact Gradient Projection
M.Sc.	Zhan Niu	Theory-guided machine learning in geophysics

Semblance-based velocity picking using unsupervised machine learning

Ninoska Amundaray and Daniel Trad

ABSTRACT

Normal moveout (NMO) correction depends on the identification of optimal velocitytime pairs to flatten the hyperbolic character associated with seismic reflections. Semblance panels are ideal attributes to accomplish this task. However, they are highly affected by the level of noise in the data and poor calculations for short offsets. These are often overcome with additional seismic attributes, which we suggest to replace with the introduction of velocity trends based on semblance. In this study, we demonstrate that our method works as an adequate filtering technique, capable to generate inputs for applications of unsupervised machine learning (ML) in velocity analysis. The performance of three different types of clustering methods known as K-Means, Gaussian Mixture Models and DBSCAN, is investigated by the identification of velocity-time pairs to guide the NMO correction in two datasets simulated for the Marmousi model. In both tests, deep reflectors are corrected independently of the clustering technique used; whereas shallow events are only flattened at near and mid offsets, and under corrected or stretch at far offsets.

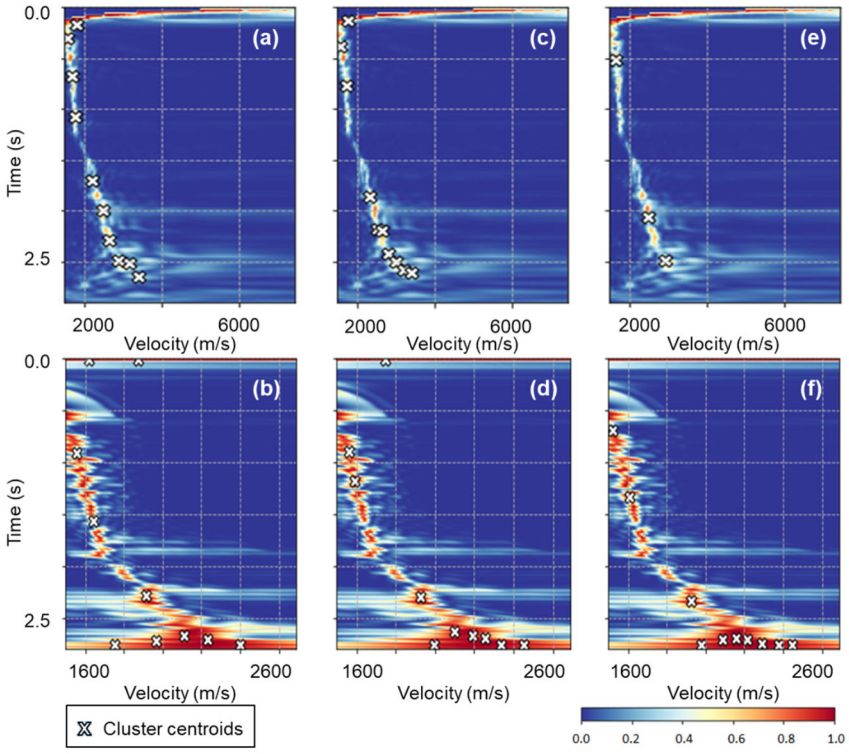

FIG. 1. Semblance panels overlaid with the identified clusters centers. Results in (a)-(b) are suggested by K-Means, in (c)-(d) by Gaussian Mixture Models, and in (e)-(f) by DBSCAN. Top row are semblance panels from Marmousi model in a shallow marine setting; whereas, bottom row are panels from Marmousi model in a deep-marine setting.

Time-lapse elastic full waveform inversion of CO_2 injection at CaMI FRS using VSP: a feasibility study

Ninoska Amundaray* and Kris Innanen

ABSTRACT

Full waveform inversion (FWI) relies on the quality and frequency content of the data to recover subsurface models. Successful applications have proven to delimit reservoirs with high-resolution models, as well as, measuring parameter variations associated to production processes. Currently, an injection program of carbon dioxide (CO_2) is being conducted at the Containment and Monitoring Institute Field Research Station (CaMI.FRS). Field data from the baseline phase has been successfully inverted for the site, and data from an advanced injection stage is expected to be recorded in the following years. Hence, there is a need to assess the extents and limitations of this technique to resolve changes in the reservoir through experiments designs consistent with settings deployed at CaMI.FRS. In this study, we examine FWI using vertical seismic profiles (VSP) with velocity-density and impedance-density parameterizations, and by two inversion strategies in the data-space for three stages of CO_2 injection. Inverted models demonstrate superior constraints of P- and S-wave variations by a sequential inversion scheme in terms of relative change between modeled stages and model misfit. Likewise, impedance-velocity is suggested as the optimal parameterization to resolve reservoir changes with approximately 2% to 4% more measured variations.

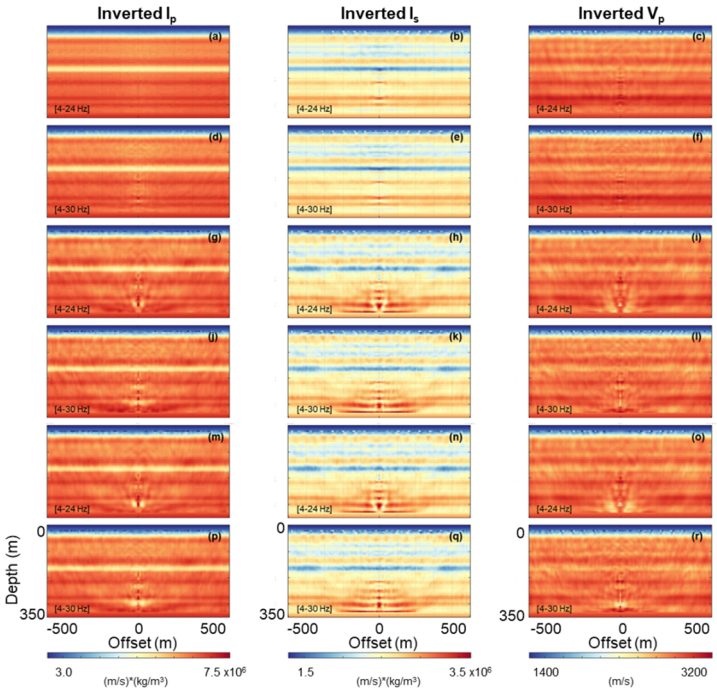

FIG. 1. Inverted models from two frequency bands for three phases of CO_2 injection using a sequential inversion strategy with impedance-velocity parameterization. (a)-(f) are the inverted baseline models, (g)-(l) are the inverted medium injection phase models, and (m)-(r) are the inverted final injection phase models.

3-D data Interpolation and denoising by adaptive weighting rank-reduction method using singular spectrum analysis algorithm

Farzaneh Bayati and Daniel Trad

ABSTRACT

A difficult challenge in seismic processing and imaging is to address insufficient and irregular sampling. Most processing algorithms require well-sampled data, which involves small sampling intervals with a regular distribution. Recently, rank reduction methods are used in seismic processing algorithms. These methods are based on rank reduction of the trajectory matrices using truncated SVD. Estimation of the rank of the Hankel matrix depends on the number of the plane waves; however, when it comes to more complicated data, the rank reduction method may fail or give poor results as a consequence of curved events not having a small rank (sparse) representation. To satisfy the plane wave assumption for the rank reduction method, one can utilize local windows to assume that events are plane waves. The rank reduction method requires the number of events as the rank parameter. This number defines the minimum rank selected in each step. In this paper, we first propose a method, which selects the rank automatically in each window by finding the maximum ratio of the energy between two singular values. The method may select a large rank to get the best result for very high curved events, which leads to remain residual errors. To overcome the residual errors, then we apply a weighting operator on the selected singular values to minimize the effect of noise projection on the signal projection. We test the efficiency of the efficiency of the proposed method by applying it to both synthetic and real seismic data.

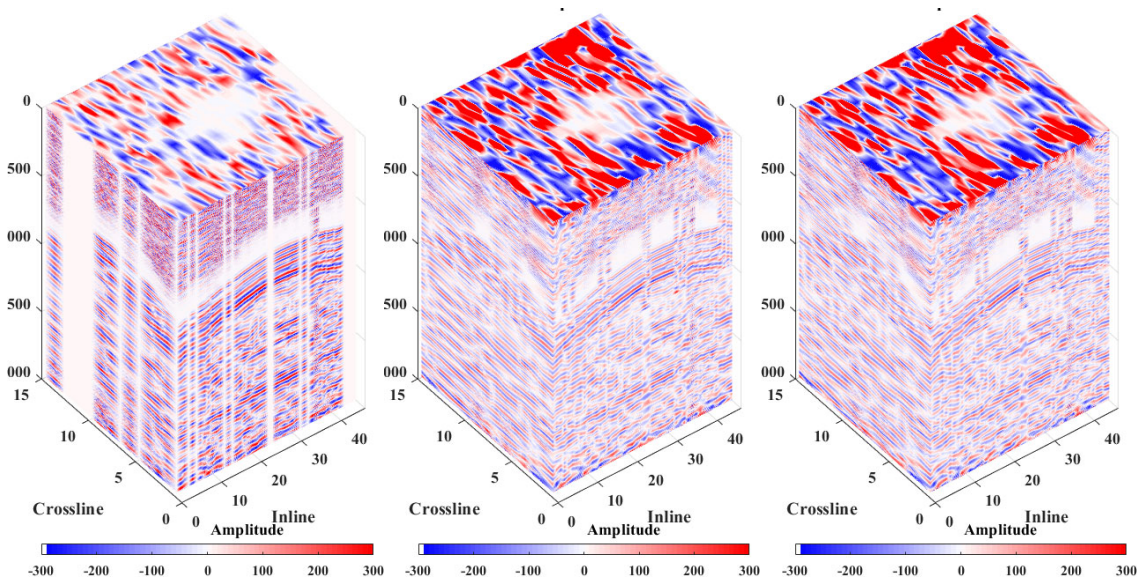

FIG. 1. a) Input real data, b) interpolation result of applying truncated SVD approach, c) interpolation result of applying adaptive weighting rank-reduction method.

2021 CREWES field work

Kevin L. Bertram, Kevin W. Hall, Malcolm Bertram, Rachel Lauer, Kris Innanen

ABSTRACT

This year has seen a return to some of the normal operations of CREWES in the field. The ability to acquire field data provides CREWES a great advantage by providing the opportunity to test theories using actual seismic data.

Field acquisition projects that were carried out in 2021 include: a) a VSP survey carried out at the CaMI.FRS; b) a thumper test using the Seismic Group's nitrogen spring thumper trailer and a truck mounted thumper from Explor; c) testing of the CREWES downhole tool; d) the 2021 GOPH549 undergraduate field school; e) timelapse during CO_2 injection at CaMI.FRS.

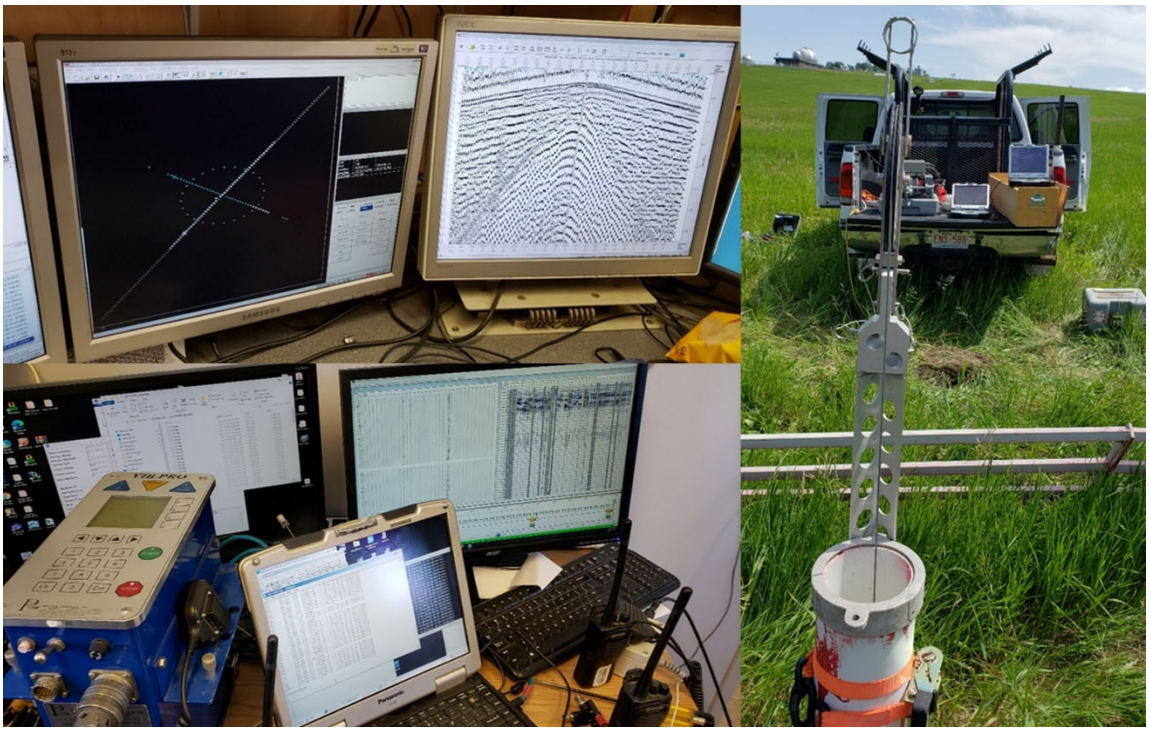

FIG. 1. Collecting data in the field..

Estimation of fracture indicators using azimuthal PP-wave amplitudes without NMO correction

Huaizhen Chen* and Kris Innanen

ABSTRACT

Seismic waveforms at large offsets is stretched during NMO correction, which are usually muted in seismic processing. However, in horizontal vertically isotropic (HTI) media or hydrocarbon reservoirs with vertical fractures, variation of seismic wave reflection with azimuthal angle is more obvious at large offsets, which means seismic waveforms of large offsets are indispensable to implement a better characterization of HTI media and fractured reservoirs. To circumvent the NMO stretching and reserve seismic waveforms at large offsets, we present an approach and workflow of employing seismic waveforms without NMO correction to estimate elastic impedance EI and fracture parameters (i.e. fracture weaknesses). Starting with re-expression of P- and S-wave velocities of HTI media, we derive PP-wave reflection coefficient and azimuthal EI as a function of the normal and tangential fracture weaknesses based on the solution of Zoeppritz equations. Using the derived azimuthal EI, we introduce a NMO operator to the convolution model to generate PP-wave seismic data without NMO correction. A two-step inversion workflow is established to estimate fracture weaknesses using seismic data, which is implemented as: 1) using seismic data without NMO correction at different incidence and azimuthal angles to invert for EI, and 2) using difference in EI at different azimuthal angles as input data to estimate fracture weaknesses. Bayesian inversion algorithm is employed in the two-step inversion. Synthetic seismic data of signal-to-noise ratio (SNR) of 2 is generated to verify the robustness of the proposed inversion approach. In the case of applying the proposed inversion approach and workflow to real datasets acquired over fractured reservoirs, reliable results of fracture weaknesses are obtained, which may guide the identification of potential fractured reservoirs.

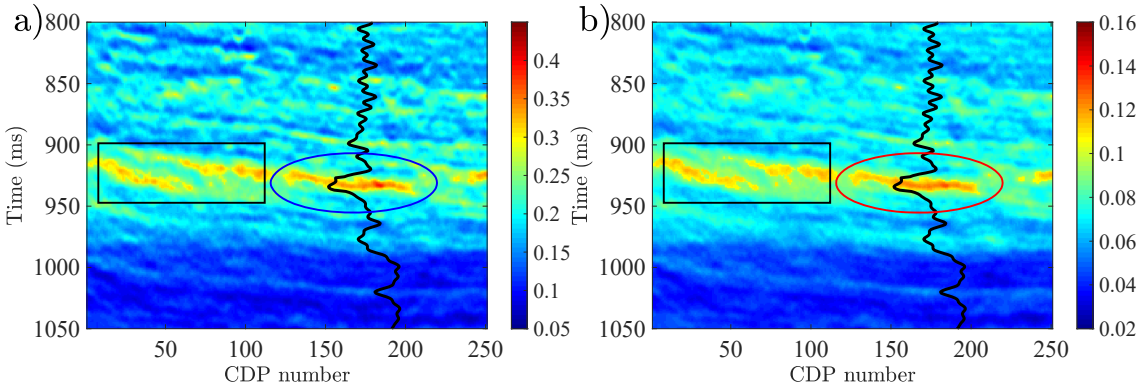

FIG. 1. a) Inversion results of the normal fracture weakness, and b) Inversion results of the tangential fracture weakness. The curve is P-wave velocity.

Inversion of SV-to-SV wave AVAZ data for fracture indicator: Synthetic example

Huaizhen Chen and Kris Innanen

ABSTRACT

Shear wave travel time analysis and reflection amplitude inversion can supply fracture estimation approaches established using P-wave azimuthal seismic data. Starting with rewriting SV-wave velocity as a function of normal and tangential fracture weaknesses in horizontal transversely isotropic (HTI) media, we present a new fracture indicator and express SV-wave velocities of two fractured layers across a reflection interface in terms of reflectivities of S-wave velocity and fracture indicator. Using the expressed SV-wave velocities, we derive SV-SV wave reflection coefficient based on a simplified version of Zoeppritz equations' solution, and we also present SV-SV wave anisotropic elastic impedance (EI) and its normalized form. Based on the derived reflection coefficient and anisotropic EI, we propose an inversion approach of employing SV-SV wave gathers to estimate unknown parameters involving S-wave velocity of background rock, density and fracture indicator, which is implemented as: 1) the least-squares inversion for anisotropic EI of different dominant incidence angles, and 2) the estimation of fracture indicator using the first- and second-order derivatives of anisotropic EI with respect to unknown parameters. We employ noise-free and noisy synthetic seismic gathers to illustrate the robustness and stability of the inversion approach, which reveals that the proposed approach may be reserved as a valuable tool for identifying fractures using SV-SV wave seismic gathers.

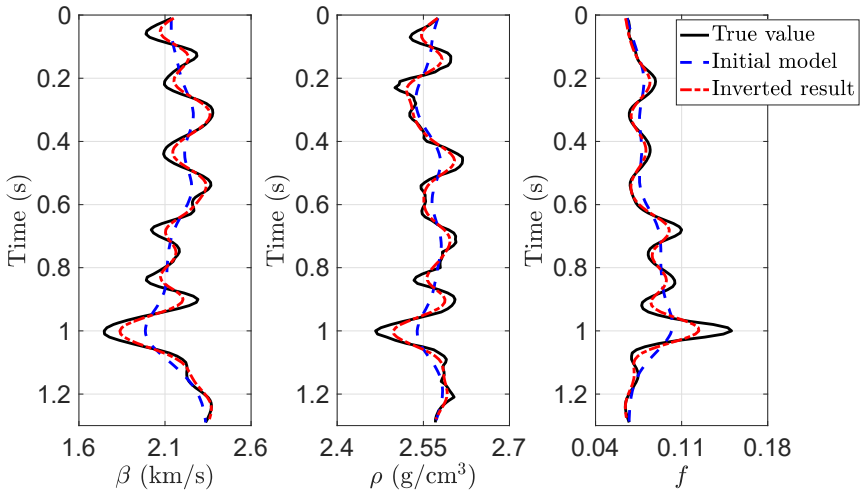

FIG. 1. Comparisons between inversion results and true values of S-wave velocity, density and fracture indicator.

Full waveform inversion of DAS field data from the 2018 CaMI VSP Survey

Matt Eaid*, Scott Keating, and Kris Innanen

ABSTRACT

Carbon capture and storage has become a key research area for diverting carbon dioxide gas away from the atmosphere by storing it in deep subsurface reservoirs. Seismic data are a key technology for monitoring the injected carbon dioxide to ensure that it remains in the target formation and does not migrate into regions where it may pose a risk. Distributed acoustic sensing permits permanent installation of receivers in borehole geometries, allowing for highly repeatable sampling of transmission wavefield modes which is crucial for seismic monitoring surveys. To fully leverage the data supplied by DAS fibers, theoretical inverse methods must transfer to DAS data acquired in the field both in isolation and in combination with accelerometer data. In 2018, the Consortium for Research in Elastic Wave Exploration Seismology acquired a 3D walkaway-walkaround VSP survey into both three-component accelerometers and DAS fiber. In this report the DAS fiber data are inverted using isotropic-elastic full waveform inversion. A method for the source wavefield estimation and a log-derived model parameterization are found to be crucial for convergence of the inverted models in FWI. Inverting the DAS data independently provides robust parameter estimates of the subsurface P-wave velocity, S-wave velocity, and density structure with a good fit between modeled and field data. However, inverting both datasets together using a newly formulated objective function that provides a means of controlling the relative emphasis on DAS and accelerometer data is shown to have a stabilizing effect on the inverted models when compared to using either dataset alone.

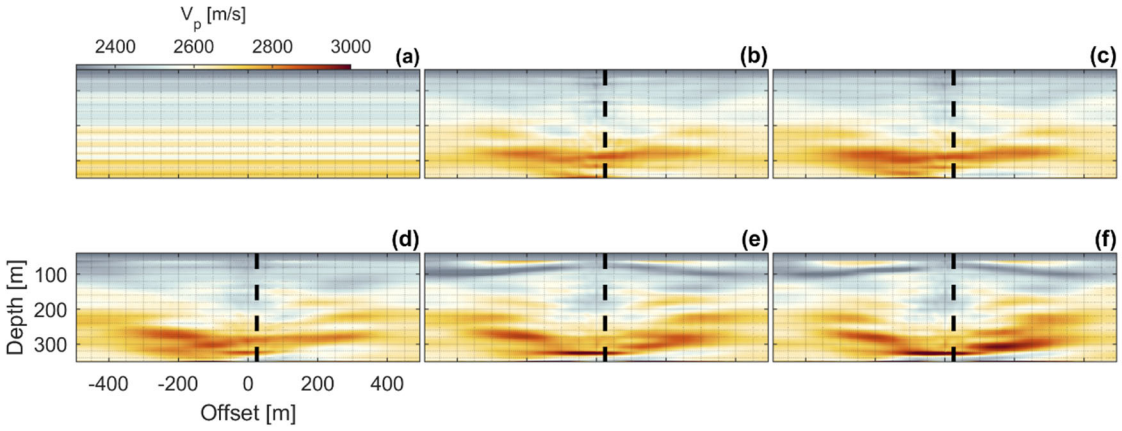

FIG. 1. a) Smoothed P-wave velocity log. Inversion results for a combined DAS-accelerometer objective function with the trade-off parameter set to (b) $\tau_D = 25\%$, (c) $\tau_D = 33\%$, (d) $\tau_D = 50\%$, (e) $\tau_D = 66\%$, and (f) $\tau_D = 75\%$. Larger values of τ_D place more emphasis on DAS data relative to accelerometer data.

Processing of the 2018 CaMI VSP survey for full waveform inversion

Matt Eaid*, Scott Keating, and Kris Innanen

ABSTRACT

In 2018, the Consortium for Research in Elastic Wave Exploration Seismology in partnership with the Containment and Monitoring Institute (CaMI) acquired a vertical seismic profile using three-component accelerometers and distributed acoustic sensing fibers. The overarching goal of CaMI is to develop technologies for the monitoring of sequestered CO_2 in a reservoir at 300 meters depth using time-lapse seismic methods. The 2018 VSP was a acquired as a baseline survey to support these goals. In this report, both the accelerometer and DAS datasets are processed to prepare them for inclusion in full waveform inversion. FWI of these two datasets will be discussed in two companion reports in this issue.

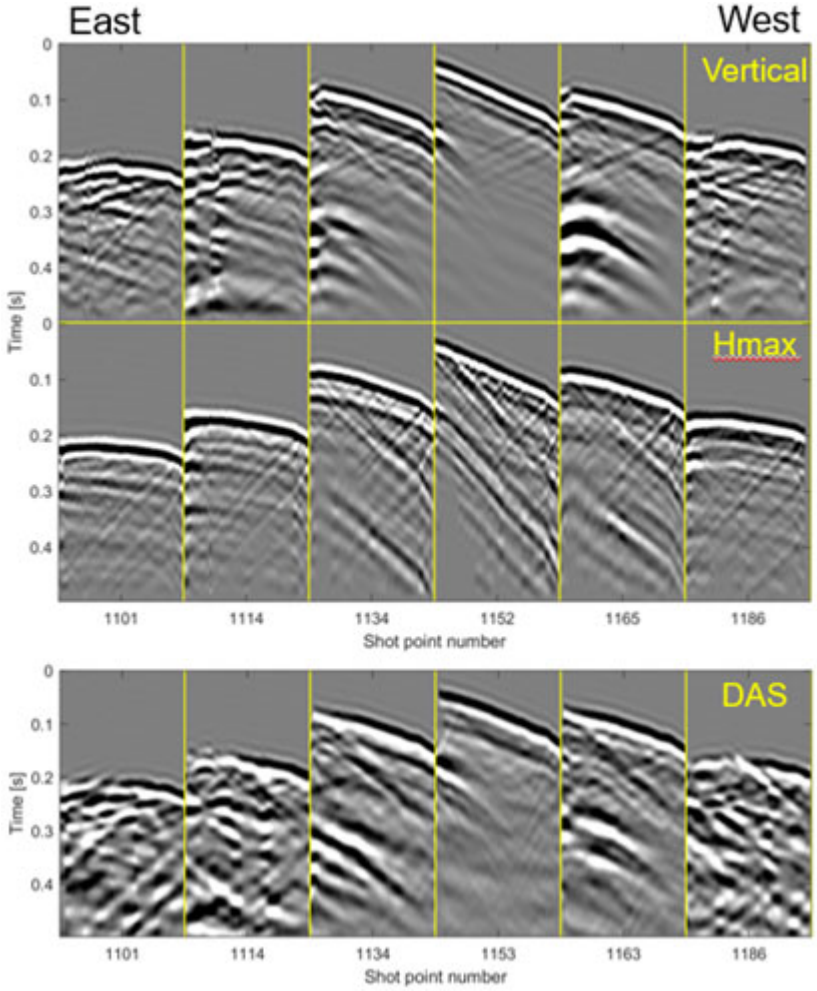

FIG. 1. Processed field data from the 2018 CaMI FRS vertical seismic profile after applying a processing workflow. The top row plots the vertical component of the accelerometer data, the middle row the Hmax component, and the bottom row the DAS data for every 13th shot point.

Reducing source wavelet non-repeatability for time-lapse shot gathers

Xin Fu and Kris Innanen

ABSTRACT

In time-lapse seismic surveys, the effective seismic signals producing by property changes of subsurface rocks are often ruined by the nonrepeatability noises. In this paper, starting from the wave equation, base on the relationship between wavefields and Green's functions, we propose two frequency-domain matching filters (f_w and f_s) to reduce source wavelet nonrepeatability for time-lapse shot gathers, one (f_w) is the spectrum ratio of the baseline and monitoring wavelets, the other one (f_s) is the average spectrum ratio of the baseline and monitoring traces. The former requires the wavelets information of baseline and monitoring data, and the latter is source-independent. After reducing the source wavelet nonrepeatability, we employ a time-shifts correction by a fast local cross-correlations algorithm to further reduce nonrepeatability errors in the difference data (monitoring data minus baseline data) that caused by time shifts between monitoring and baseline data. And then, a reverse time migration (RTM) in depth with a Poynting Vector imaging condition is used to reduce the remaining errors arising from the inaccuracy of the source-independent matching filter. The feasibility of our methods is demonstrated by the synthetic noise-free and noisy data tests. The spectrum ratio of the baseline and monitoring wavelets can effectively solve the source wavelet nonrepeatability issue. The source-independent filter also shows good performance during these tests.

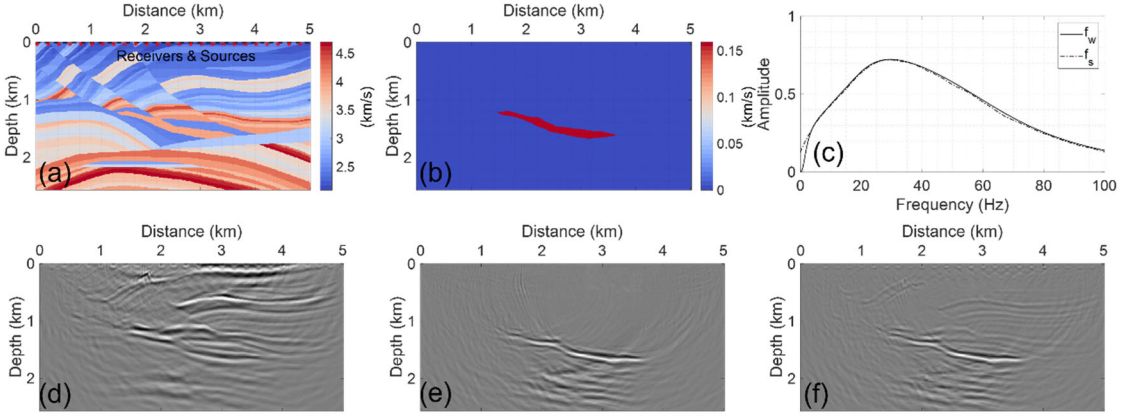

FIG. 1. (a) Baseline model (acoustic) and acquisition geometry. (b) Time-lapse model. (c) Frequency-domain filters, f_w and f_s, to reduce source wavelet non-repeatability for time-lapse shot gathers. (d)-(e) are RTM images of difference data (monitoring data minus baseline data) after time-shifts corrections using all shots. (d) Baseline and monitoring wavelets are different, and monitor data are not processed. (e) Baseline and monitoring wavelets are different, and monitoring data are filtered by f_w. (f) Baseline and monitoring wavelets are different, and monitoring data are filtered by f_s.

Stepsize sharing in time-lapse full-waveform inversion

Xin Fu* and Kris Innanen

ABSTRACT

Full waveform inversion (FWI) methods can produce high-resolution images of the physical properties of the subsurface. It has become a powerful tool for time-lapse or 4D seismic inversion, with applications in the monitoring of reservoir changes with injection and production, and potentially long term storage of carbon. Current time-lapse FWI strategies include the parallel strategy (PRS), the sequential strategy (SQS), the double-difference strategy (DDS), the common-model strategy (CMS), and the central-difference strategy (CDS). PRS time-lapse inversion is affected by convergence differences between the baseline and monitoring inversions, as well as non-repeatable noise and non-repeatable acquisition geometries between surveys. The other strategies above are largely efforts to fix these sensitivities of PRS. In this paper, we introduce and examine two strategies, which we refer to as stepsize-sharing PRS (SSPRS) and stepsize-sharing CMS (SSCMS). As the name suggests, they are characterized by a sharing of update stepsizes between baseline and monitoring stages of the time-lapse FWI. Synthetic data tests indicate that stepsize-sharing reduces artifacts caused by the PRS convergence variability. In particular, the stepsize-sharing common-model strategy (SSCMS) appears to be adept at reducing artifacts caused by all of convergence differences, non-repeated noise, non-repeatable source locations, and biased starting models. This breadth of robustness does not appear in any of the other approaches tested. Especially given that SSCMS through its sharing incurs half of the computational cost of CMS and CDS, we regard the workflow as being worth further study.

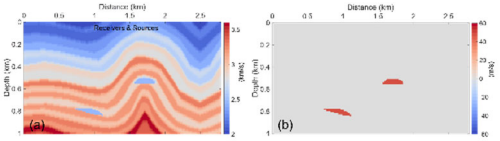

FIG. 1. True baseline model (a) and (b) time-lapse model.

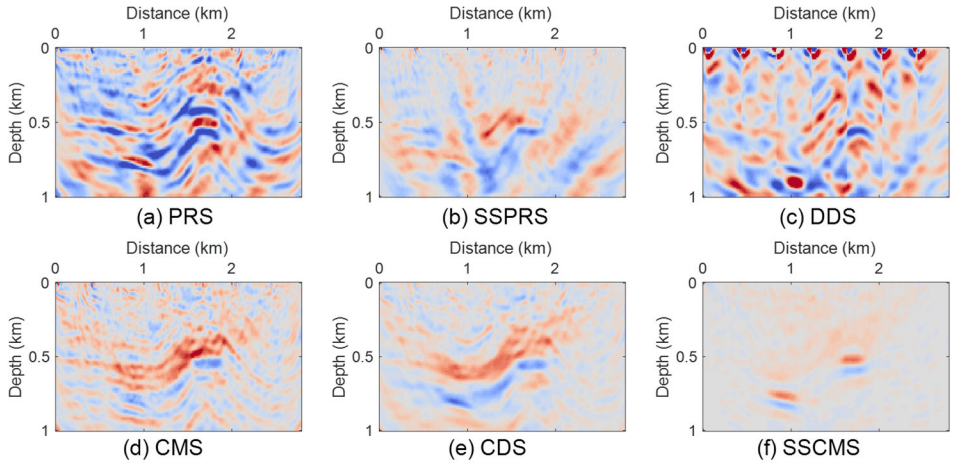

FIG. 2. Inverted time-lapse results of different strategies in the case of SNRs for both baseline and monitor data sets are 20, the monitor source locations are 10m larger than baseline source locations, and starting model is 100m/s larger than the unbiased one.

Calgary's municipal buildings energy consumption analysis and forecast

Marcelo Guarido, David J. Emery, Daniel Trad, and Kris Innanen

ABSTRACT

CO_2 emissions are pointed to as the main cause of Global Warming, and countries around the world are working to reduce their domestic emissions. Canada set to get to zeronet emissions by 2050 and is taking action on different fronts. Although the emissions per capita are reducing, the absolute emissions of the country are still increasing over the years. As part of the country's efforts, the Government of Calgary has set the same goal. We analyzed the Calgary corporate buildings data, which contains energy consumption from different types of municipal facilities and pointed that the overall electricity consumption in the city is declining, while natural gas consumption seems to be following an opposite trend. As a decision-making tool, forecasting models can predict what will be the future energy consumption. However, for that, more complete data is required, containing not only the energy consumption of each building but as well structural information about the same. We performed forecasting of global electricity and natural gas consumption using three different models: SARIMA + XGBoost, Facebook Prophet, and MARS. The first one showed to behave better with the seasonality and outliers, predicting a steady reduction of electricity consumption for the next three years, while the natural gas consumption will, if no action is taken, continue at the same level. Lastly, we did the impact analysis of the reduction of electricity consumption of the Calgary streetlights since 2016, due to an action of the Government of Calgary to change the light bulbs to more energy-efficient ones and estimated that the savings are feeding the equivalent of more than 5000 houses in Alberta.

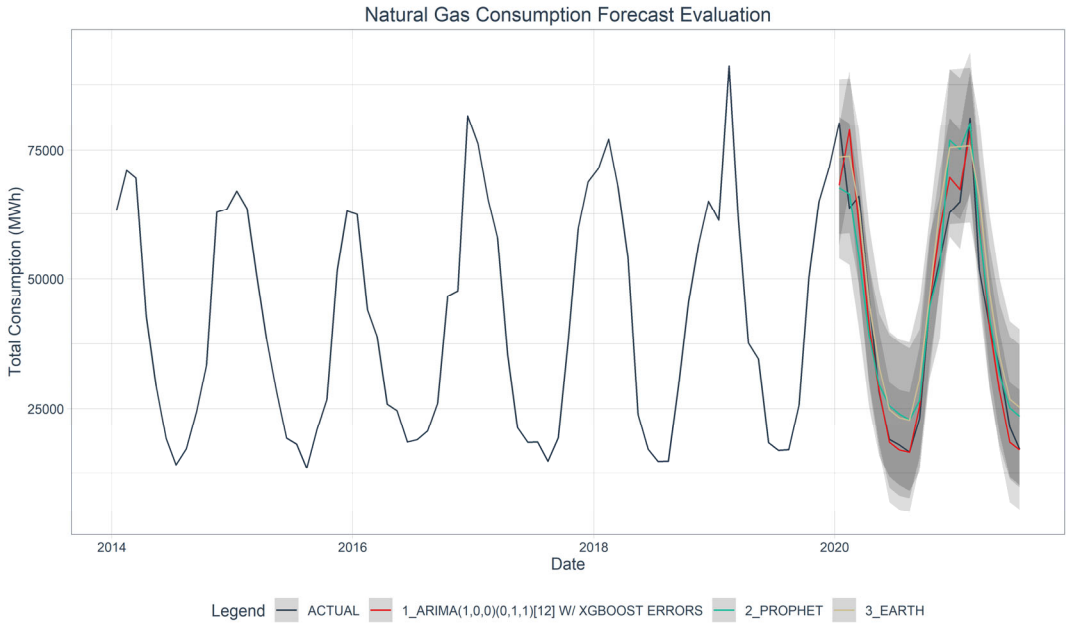

FIG. 1. Natural gas forecasting for the next 3 years.

An Overview of the Geothermal Energy Technologies

Marcelo Guarido, David J. Emery, Daniel Trad, and Kris Innanen

ABSTRACT

Geothermal resources have been used by hominids since prehistoric times for bathing, curing wounds, and tempering hunting weapons. Even religious connections are observed in old civilizations. District heating application appeared in France during the 15th century, while the first power plant was installed in Larderello, Italy, in 1913. Since then, power plant technologies and optimized geothermal resources are studied for large-scale renewable energy generation. Power plants require water temperature ranging from 95ºC to over 200ºC. Hydrothermal resources, presenting manifestations in the surface as geysers, hot springs, and fumaroles, can provide water or steam over 150ºC. With crust's gradient temperature averaged as 30ºC/km, resources in dry rock systems come from 3 to 7 km depth. But the gradient varies on the crust, and some areas are more suitable for implementation of Enhanced Geothermal Systems or closed-loop systems. With over 458,000 wells connected to the oil and gas industry, Alberta, Canada, has a high potential to reuse part of those wells, around 7,900 wells, for electricity generation if converted to EGS or closed loop. SE and E areas of the province showed the potential to reach electricity generation temperatures at depths lower than 1 km.

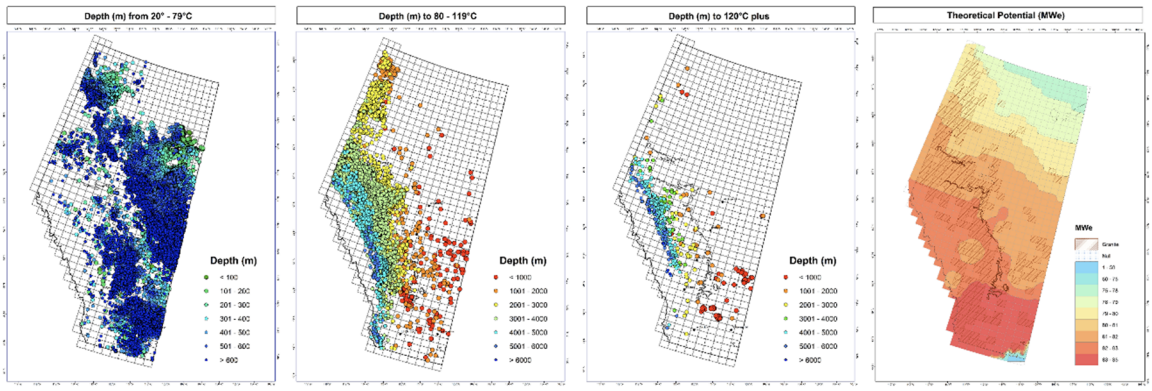

FIG. 1. Temperature per depth and Alberta's theoretical potential.

Seismic inversion with Gradient Boosting

Marcelo Guarido*, Luping Qu, Zhan Niu, Kai Zhuang, David J. Emery, Daniel Trad, and Kris Innanen

ABSTRACT

Geophysics in the Cloud promoted a competition with the proposal to use machine learning algorithms to perform seismic inversion. The provided data showed to be challenging, due to the small number of well logs to train the model. During the competition, most of the competitors based their strategies using deep learning models (CNN, RNN, LSTM, etc). Our proposal was to evaluate the possibility of seismic inversion using more classical and simple approaches, hence the choice of the Gradient Boosting algorithm. Predictions of P and S impedances and density using an XGBoost model are stable and strongly rely on the trend features and use seismic traces to include low to mid-frequency content. Testing neural networks structures from Scikit-Learn and Tensorflow resulted in noisy and spiky inversions, pointing to overfitting and their instability drew attention to the issue of the small number of logs for training.

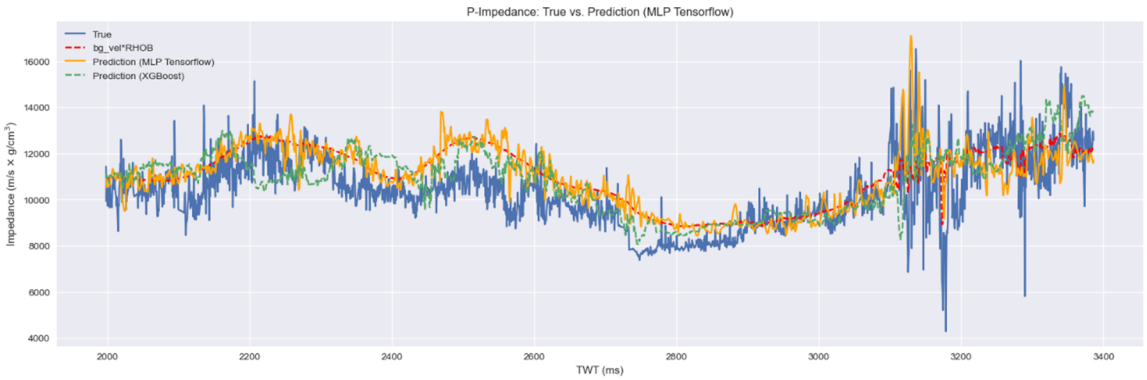

FIG. 1. P-impedance (I_P) prediction using Tensorflow (orange), P-impedance prediction from XGBoost (green), true P-impedance (blue), and background P-impedance (red).

Fibre trace registration by cross-correlations – can we successfully predict helically wound fibre pitch from recorded data?

Kevin W. Hall*, Don Lawton, and Kris Innanen

ABSTRACT

The Containment and Monitoring Institutes Field Research Station (CaMI.FRS) contains an approximately 5 km long optical fibre loop comprised of straight fibre cables and helically wound fibre cables that are spliced together end-to-end. The fibre loop traverses two wells, observation well 1 (OBS1) and observation well 2 (OBS2), and a 1 km horizontal trench along the surface with straight and helically wound fibre cables. We have interpolated fibre trace co-ordinates in the past for a walk-away/walk-around VSP (Snowflake) using GPS surveys, downhole gyroscope surveys, the nominal helical pitch angle (26.2°), and index of refraction corrections, but it was never entirely clear if we were using the correct helical trace spacing, or which coordinates should be assigned to what DAS trace. Quality-control checks performed by interleaving straight and helical fibre traces using interpolated coordinates plus arbitrary channel assignment shifts showed that the calculated helical fibre trace spacing was close, but not correct. In this report, we use cross-correlation to find the best match between traces in two co-located seismic datasets and apply linear regression to those results. The slope from the linear regression can be used to estimate a pseudo-pitch angle. It can also be used to estimate an unknown trace spacing (eg. helical fibre) if the other dataset has a known trace spacing (eg. straight fibre). The slope and intercept from the linear regression can also be used to register datasets by, for example, predicting helical channel numbers (fractional) that match straight fibre channel numbers. We may now interleave the datasets using the predicted channel number as a quality-control check. Additionally, if we find near integer predicted channel numbers, we can use those to anchor interpolated co-ordinates for geometry assignment.

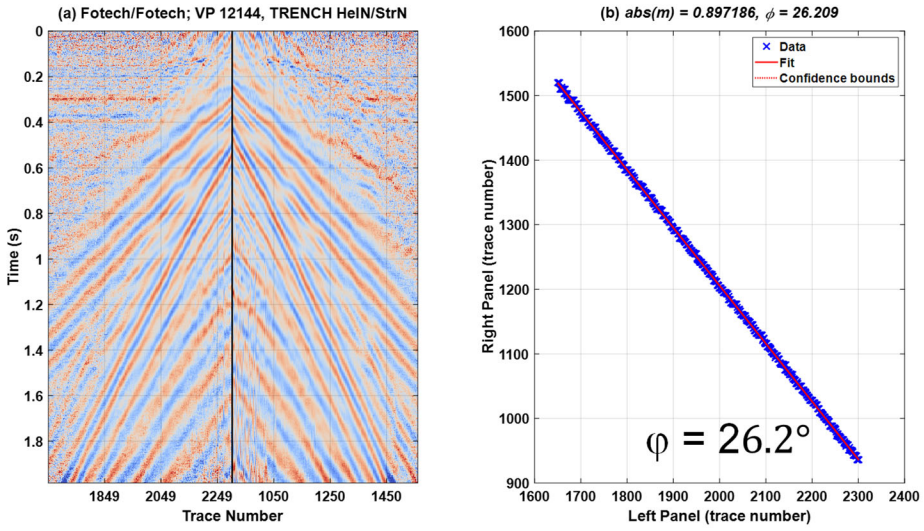

FIG. 1. Linear regression of channel numbers results from cross-correlation of straight and helical fibre data from the CaMI.FRS trench gives an estimated pseudo-pitch angle of 26.2°.

Preliminary processing of physical modeling data from circular arrays

David C. Henley

ABSTRACT

Physical modeling can be used to study many different problems where measurements of acoustic or elastic waves are used to obtain basic information about the object or target being investigated. The current physical modeling system developed and operated by CREWES has been used in many studies of elastic wave propagation suggested by various projects in the real world of seismic exploration, as well as those in wave propagation theory. In the present study, we exchange the world of seismic exploration for that of medical imaging, with the hope that methods developed for seismic imaging can be used to enhance images used for medical diagnosis.

Many novel transducer arrangements are possible for imaging targets in a physical modeling tank. We describe here some early developments in the processing used to extract useful target information from a physical model for which the acquisition geometry consists of a circular array of discrete receivers surrounding an unknown target, with sources positioned on the same circle as the receivers. Each source gather consists of recorded signals from all the receivers on the circular array accessible to that source, constrained by the mechanical limitations of the modeling system. Essentially, this experiment attempts to extract the 2-D shape of the object enclosed by the array, using principles of transit-time tomography and back-projection. Since target information in this experiment consists of variations of direct-arrival transit times from those expected for an empty circular array, the processing efforts are aimed at detecting those variations, projecting them as "shadows", and using various geometric processing tricks to combine the shadows in the source gathers to form a crude image of the target, for use as the starting point in a FWI procedure. Figure1 shows our first attempt to image a target within a circular array using projection shadows created from the target transit time anomalies.

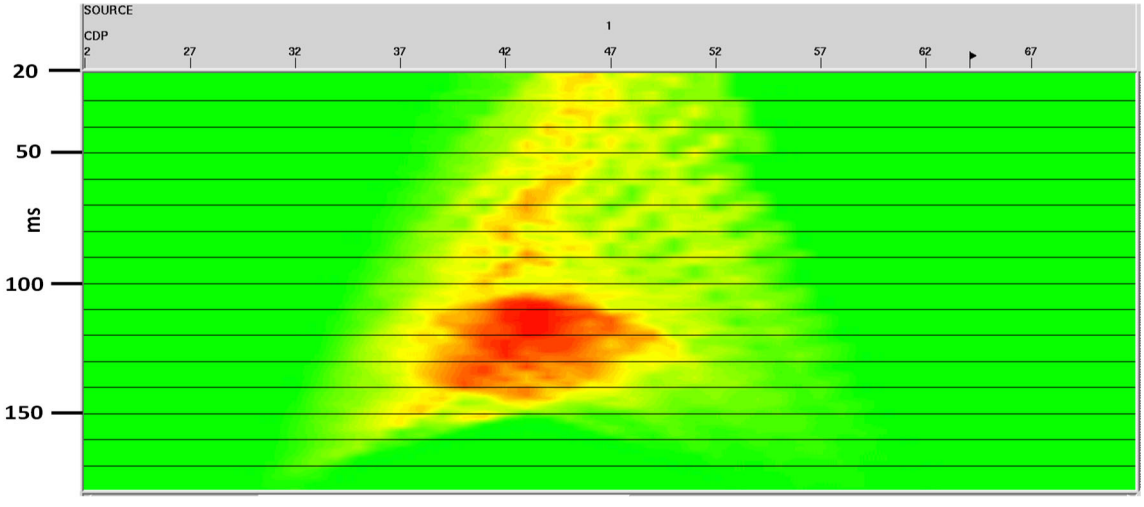

FIG. 1. First attempt at imaging projection shadows from target transit time anomalies in a circular array. Coordinates need to be converted to cartesian coordinates.

Rock physics analysis of well-log data

Qi Hu*, Kris Innanen, and Marie Macquet

ABSTRACT

We present a rock physics workflow based on the soft-sand model to convert reservoir properties (e.g., porosity, lithology, fluid saturation, and pressure) to seismic elastic attributes (e.g., velocity, density, and modulus) at the CaMI Field Research Station, Alberta, Canada. This model is selected based on the geological setting of the study region and its visible fit to the well-log data. We use the constructed rock physics model to predict the shallow section of velocity and density logs that are missing. The result shows a good agreement with the local geology. We further carry out sensitivity studies for the estimation of reservoir properties from seismic attributes. This is a nonlinear inverse problem, and we solve it using a directed Monte-Carlo method (neighborhood algorithm). Various input data parameterizations and model parameterizations are considered. We illustrate that most reservoir properties are difficult to estimate when the inversion system is underdetermined with non-unique solutions. To obtain accurate estimates, it is best to include enough input data or focus on limited solid and fluid phases by making appropriate assumptions on the others. Because the rock physics model used in the study is validated using well data, our analysis should be applicable to the regional area centered on the well.

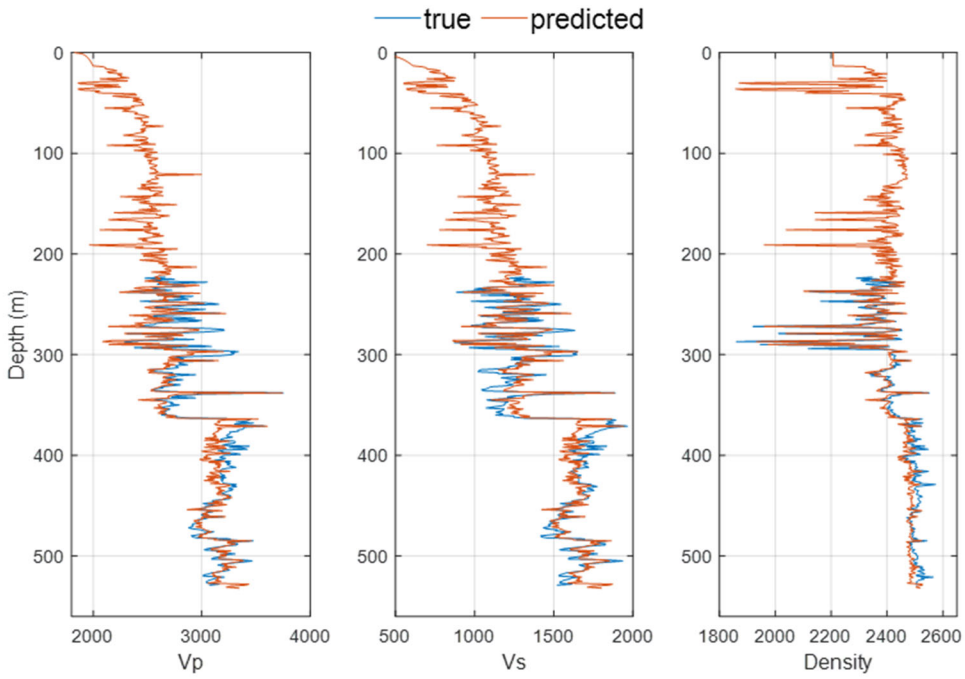

FIG. 1. Predicted velocity and density logs versus real logs. The rock physics model is then used to construct the missing logs at shallow depths.

Time-lapse rock physics CO_2 monitoring with FWI

Qi Hu* and Kris Innanen

ABSTRACT

Carbon capture and storage is a viable greenhouse gas mitigation technology. Monitoring of the injected CO_2 should, in addition to locating the plume, provide quantitative information on CO_2 saturation. We propose a full waveform inversion (FWI) algorithm for the prediction of the spatial distribution of CO_2 saturation from time-lapse seismic data. The methodology is based on the application of a rock-physics parameterized FWI scheme that allows for direct updating of reservoir properties. We derive porosity and lithology parameters from baseline data and use them as input to predict CO_2 saturation from monitor data. The method is tested on synthetic time-lapse data generated for the Johansen formation model. The results with realistic initial models and noisy data demonstrate the robustness of our approach for reconstructing baseline models. For the inversion of monitor data, we show that both the errors in baseline model estimates and the random noise could compromise the reconstructed CO_2 saturation model. We propose to improve the result using a regularization technique that consists of two penalty terms: the Tikhonov term to ensure smoothness and the prior model term to help the convergence towards expected models.

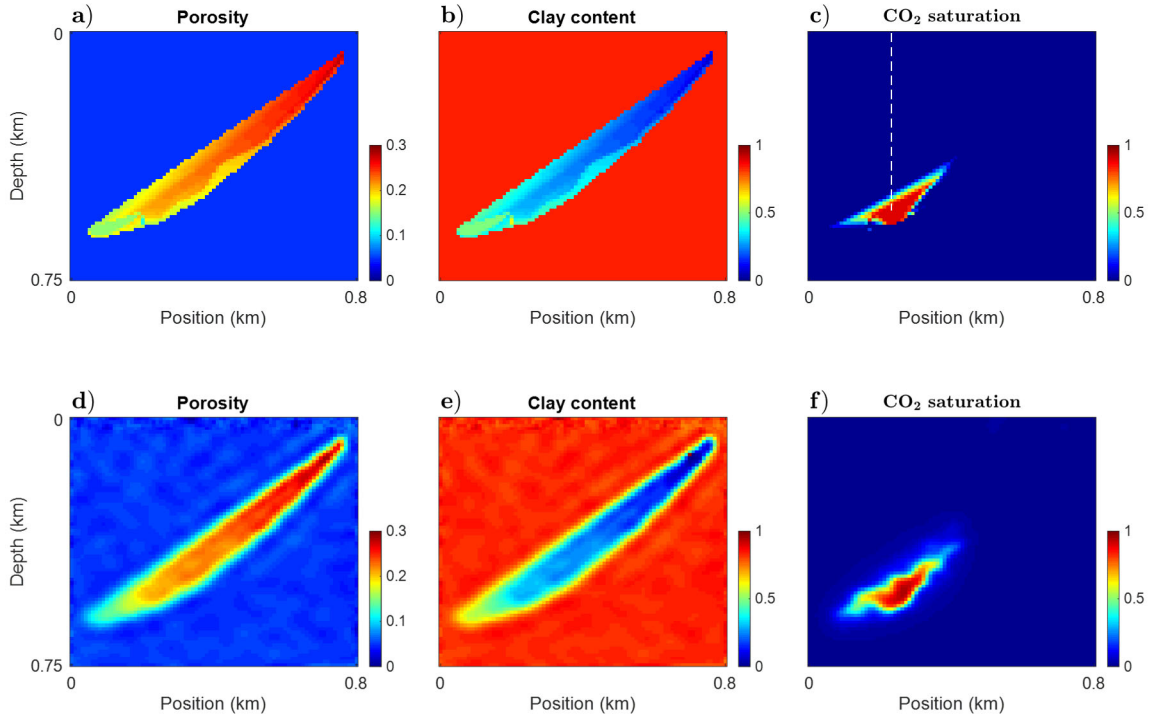

FIG. 1. (a-c) True porosity, clay content, and CO_2 saturation models.(d-f) Recovered porosity, clay content, and CO_2 saturation models. The signal-to-noise ratio is 10 for both baseline and monitor surveys. The white dashed line denotes the location of the injection well.

1D convolutional neural network with stacked bidirectional long short-term memory for seismic impedance inversion

Shang Huang, Paulina Wozniakowska, Marcelo Guarido, David J. Emery, and Daniel Trad

ABSTRACT

The seismic impedance inversion problem is ill-posed and nonlinear because of insufficient data, and is limited by wavelet estimation and frequency band-limited data. A machine learning long short-term memory algorithm (LSTM) can capture long-term dependencies so that it can work with long and densely sampled well log data to eliminate these limitations and take advantage of the known rock physics trend with depth. In this work, two models including the stacked bidirectional long short-term memory (SBDLSTM) recurrent neural network, and 1D convolutional neural network (CNN) with stacked BDLSTM have been applied to the inverse problem P-impedance and S-impedance calculation. Near, mid, far offset seismic data, migration velocity and well log data attributes are provided to generate the training set. Extreme gradient boosting (XGBoost) is used as the baseline model for comparison. Results show that SBDLSTM can predict impedance more accurately than the XGBoost method in some rapidly changing layers. 1D CNN with stacked BDLSTM can also calculate a high-frequency impedance prediction with fewer artifacts. The promising aspect is that both SBDLSTM and 1D CNN with SBDLSTM approaches can maintain a good fit when given a small number of training datasets.

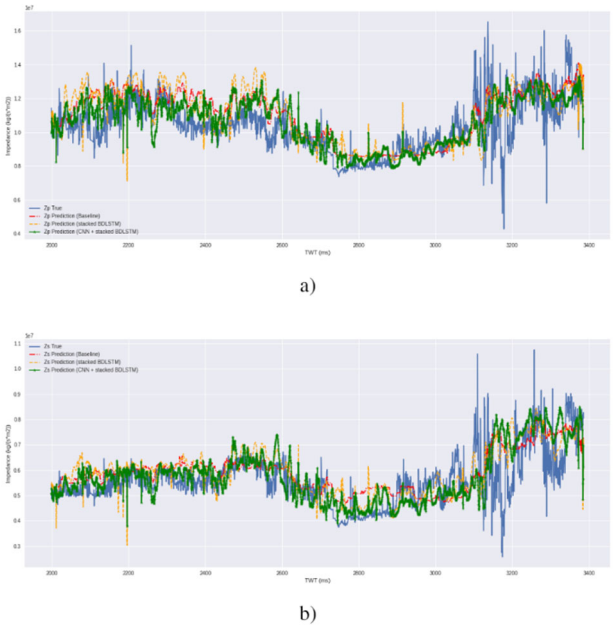

FIG. 1. Testing well for (a) P-impedance and (b) S-impedance: true value (blue), XGBoost prediction (red dashed line), stacked BDLSTM prediction (orange dashed line) and 1DCNN-SBDLSTM prediction (green solid line). 1DCNN-SBDLSTM can help suppress the artifacts by the CNN feature extraction and recover the lithology variance caused by rapid impedance amplitude change.

Convolutional neural network-based reverse time migration with multiple energy

Shang Huang* and Daniel Trad

ABSTRACT

Reverse time migration (RTM) with multiples has the advantage that it can handle steeply dipping structures and offer high-resolution images of the complex subsurface. However, there are some limitations on the initial model chosen, aperture illumination and computation efficiency. Reverse time migration has the dependency on reliable initial velocity models. If the input background velocity model is smoothed or not accurate, the RTM result image will have poor performance. RTM with multiple energy (RTMM) can help improve the illumination but will generate crosstalks because of the interference between different orders of multiples. One solution is to apply least-squares reverse time migration, which updates the reflectivity and suppresses artifacts through iterations. However, the accuracy still depends heavily on the input and the computation time is costly. We proposed a method based on a convolutional neural network (CNN) that behaves like the filter in LSRTM but is more efficient. This approach can learn patterns or features from geological structures and predict reflectivity by some smoothed velocity models through a modified residual U-Net, trained to improve the quality of RTM images. Numerical experiments show that RTMM-CNN can recover major structures and thin layers with high resolution and accuracy compared with RTM-CNN.

(1) (2)

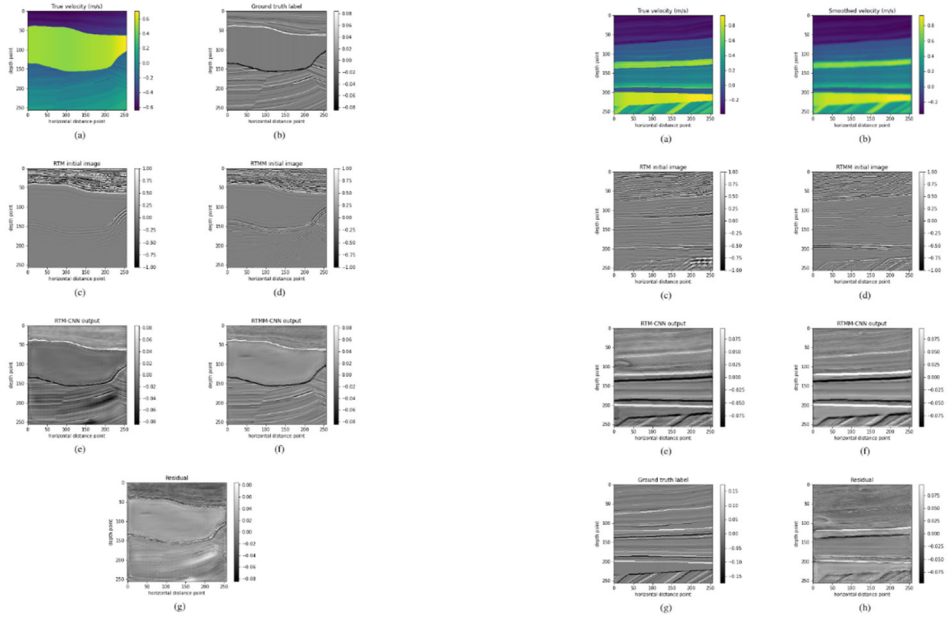

FIG. 1. (1) Train set extracted from the Pluto model and (2) test set generated from the Marmousi model. (1)a and (2)a give true velocity models after scaling. (1)b and (2)g denote the ground truth label for reflectivity coefficient, and (2)b is the smoothed velocity after scaling. Both (1)c-f, and (2)c-f represent the RTM image, RTMM image, RTM-CNN output and RTMM-CNN output separately based on the input set. (1)g and (2)h provide the residual between (f) and (e).

Phase shift plus interpolation migration with scattering terms

Shang Huang and Daniel Trad

ABSTRACT

The phase shift plus interpolation (PSPI) algorithm is a useful tool to directly solve the scalar wave equation. The results have the natural properties of the wave equation. One common issue is PSPI migration is aperture limited. In this paper, we proposed an approach that extends the illumination by adding the scattering term in PSPI migration. The benefit is keeping the input the same which means this method does not need to estimate or modify the shot records. Iteratively adding the scattering term for each boundary layer. Numerical examples show that this improved method can recover broader illumination, for example, the horizontal events and dome structures, compared with using PSPI migration only.

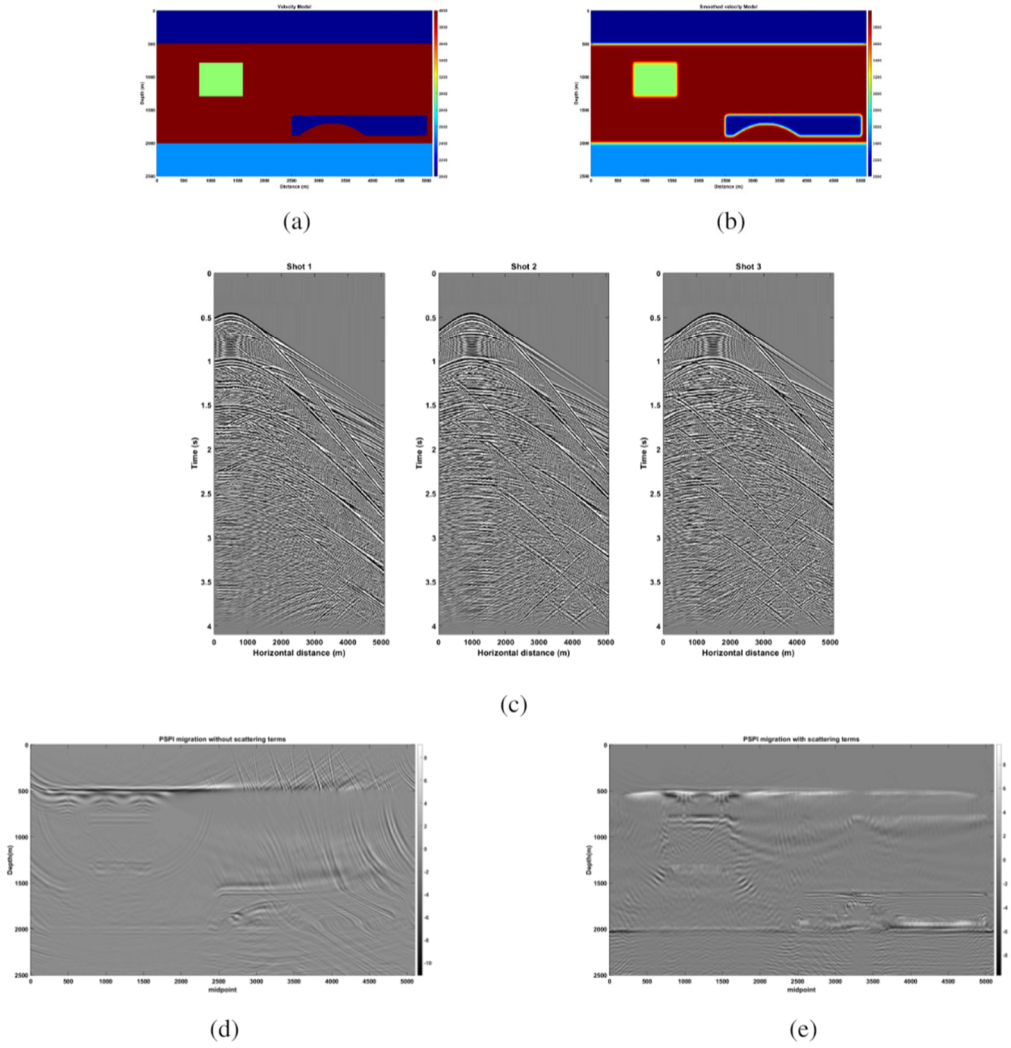

FIG. 1. (a) True horizontal-layered velocity model. (b) Smoothed horizontal-layered velocity model. (c) Shot records where the shots are located on the surface at 500, 1000 and 1500 meters respectively. PSPI migration (d) without scattering term and (e) with scattering terms.

Navigation in a model space with misfit-induced curvature

Kris Innanen

ABSTRACT

We investigate the consequences in inversion of adapting our geometrical picture of model space. We consider that model space is curved by the presence of the misfit or objective function. Within such a space, the simplest possible curves, equivalent to straight lines in flat space, are geodesics. Paths are normally followed by model estimates in the process of updating and in estimating uncertainty, and we examine the geodesics with this in mind --- is it possible that visiting points in model space in the order determined by a geodesic is a valuable exercise? There are some hints that the answer may be yes. Geodesics computed with coordinates with lower (covariant) indices appear to orbit regions of model space surrounding the minimum of the objective function in a manner which may have application in uncertainty evaluation.

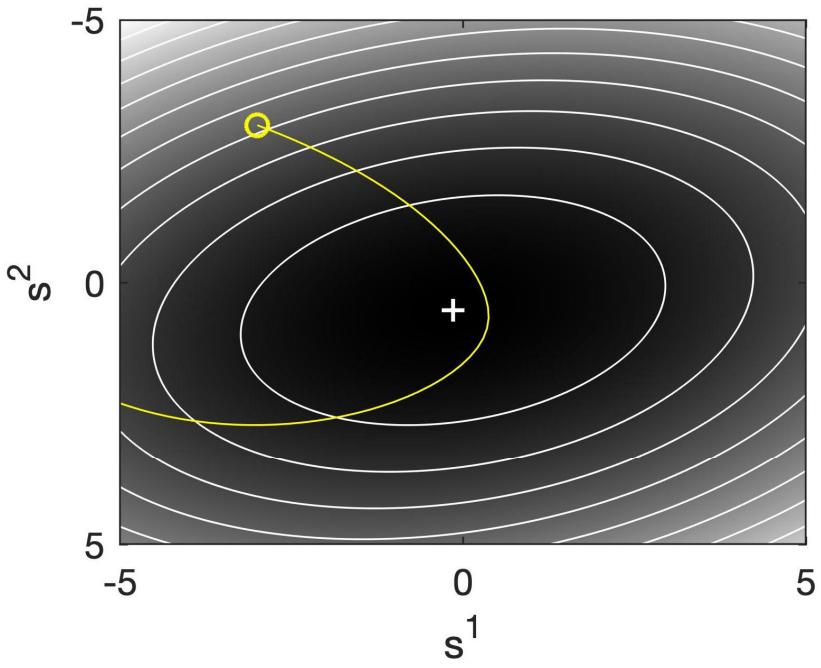

FIG. 1. An example geodesic in a 2-parameter model space curved by a quadratic objective function. Can these paths be tuned and calculated to characterize the uncertainty of this inverse problem?

A phase transition in the O'Doherty-Anstey model

Kris Innanen

ABSTRACT

In the O'Doherty-Anstey (OA) model, a stack of interfaces redistributes the amplitude of a transmitted wave pulse across a range of lags, and does so more and more widely as the reflectivities and number of interfaces grow. This is suggestive of a Maxwell-Boltzmann statistical model involving an ensemble of weighted raypaths, with a particular raypath and its weight playing the role of a system microstate, and lag playing the role of the energy. An artificial temperature, in the same units as the lag, is introduced, which measures in a bulk sense the reflection strengths and interface numbers in the stack. The partition function for such a model requires an estimate of the degeneracy of these states at each lag, which we argue is provided by one of the intermediate calculations in the OA model. Seeded by a real or simulated reflectivity series, a numerical estimate of the partition function allows the average lag to be calculated as a function of temperature. A critical transitional region dividing two distinct temperature regimes (one in which pulses are dominated by small lags and one in which pulses are dominated by lags of roughly the length of the input reflectivity) is observed.

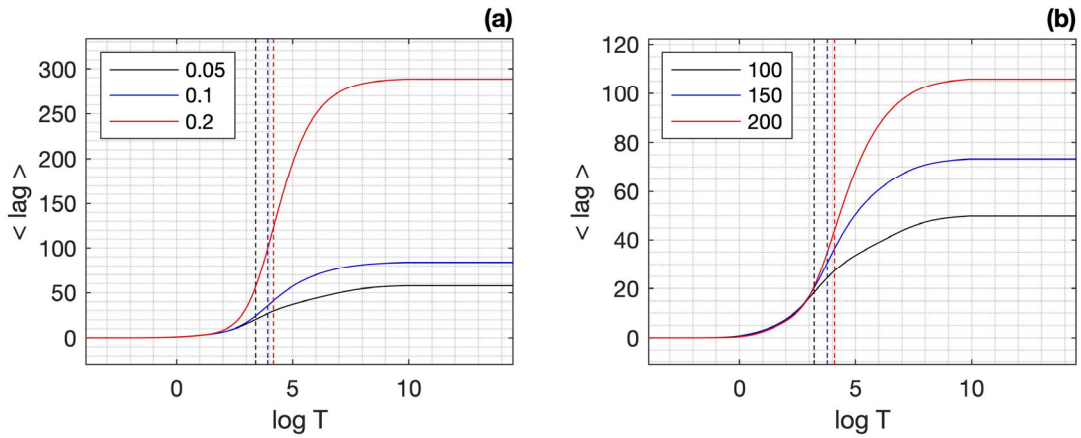

FIG. 1. Plots of ⟨l⟩ versus the logarithm of the lag-temperature T (solid), with points of maximum change identified as transition points (dashed). (a) Three curves corresponding to increasing reflectivity values, with standard deviations of 0.05 (black), 0.1 (blue), and 0.2 (red). (b) Three curves corresponding to increasing reflectivity series length, with 100 points (black), 150 points (blue), and 200 points (red).

Quantifying uncertainty in tomographic problems with a statistical zipper model

Kris Innanen

ABSTRACT

The statistical "molecular zipper" model used by Kittel to analyze the unraveling of a strand of DNA and its relationship to temperature is ported to the problem of analysis of uncertainty and appraisal in tomographic inversion. Equilibrium methods due to Boltzmann, with an emphasis on the analytically-derived partition function of the zipper, are used to estimate the average contribution of a tomographic cell to the bulk properties of the data. This number is seen to depend on almost all features of the experiment we expect to impact the reliability (or at any rate the importance in explaining the data) of each cell of a tomographic model individually. Specific techniques for analyzing this number, and spatial maps of the number, especially as it varies with an artificial temperature (whose value reflects broadly fast versus slow geological structures), remain to be created.

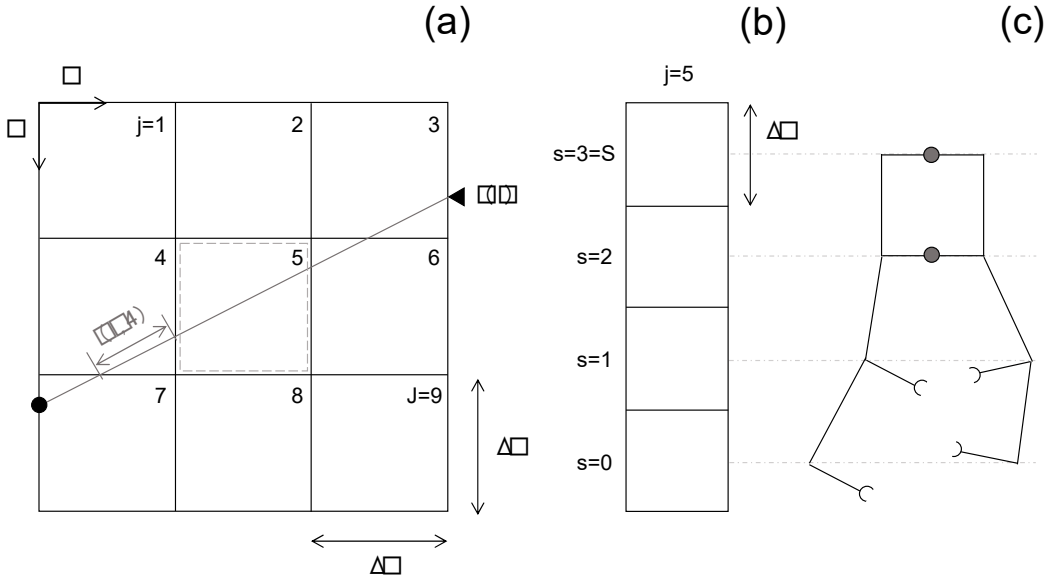

FIG. 1. (a) A coarse slowness grid, with cells numbered j = 1,...,J. An example source and receiver pair, and their ray, are illustrated. Traveltime along the ray gives the ith datum τ(i). The ith ray has a length l(i, j) in the jth cell; the l(i, 4) segment is illustrated. (b) Each cell (e.g., j = 5) is assigned a discrete slowness. In this case s = 1, giving the impression of a pile of bricks, two bricks in height. (c) The brick pile plays the role of the molecular zipper, e.g., "2 bricks" ~ "2 broken zipper links".

A selective review of methods of statistical mechanics

Kris Innanen*

ABSTRACT

Elsewhere in this report we make some suggestions about the use of statistical - mechanical models to assess geophysical inverse problems. Computational difficulties appear in general when the Boltzmann theory is applied to real-world problems, with only a relatively small number of problems giving rise to summable series and closed-form solutions. So, our approach has been to start from well-known models that have been shown to be mathematically tractable, and press these into geophysical service. (If this proves to be a valuable exercise, expending the resources to solve more computationally involved versions may then be justifiable.) In this review, we set up some of the ideas and concepts of statistical mechanics, as well as the basics from which we establish and analyze models. Then, we review several relevant models, some with the aim of exemplifying the rules, and others because of their possible use in geophysics. The latter class includes especially (or so it seems at present) the molecular zipper and the law of atmospheres.

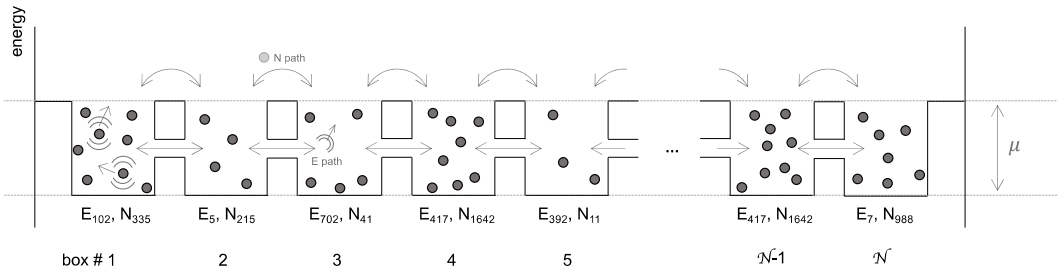

FIG. 1. The ensemble is a suite of replica systems set up to interact with one another. If the systems interact thermally, or exchange energy, and interact chemically, or exchange particles, the suite is referred as the grand canonical ensemble. If those interactions are restricted to involve energy exchanges only, it is instead referred to as the canonical ensemble.

The statistical mechanics of model space shuttles

Kris Innanen

ABSTRACT

Null space shuttles are an artifice which help quantify uncertainty in seismic full waveform inversion. Recent papers have framed these shuttles in terms of artificial dynamical systems, in which high-dimensional orbits are computed in a potential produced by the objective function. Here we pursue a natural extension of this, which is to develop a barometric equation for gases of these shuttles. This paper is largely mathematical, and ends with that equation. The main effort is in developing an approach based on the eigenvalues of the shuttle mass matrix and the Hessian matrix to produce a closed-form (if yet computationally expensive) expression for the partition function.

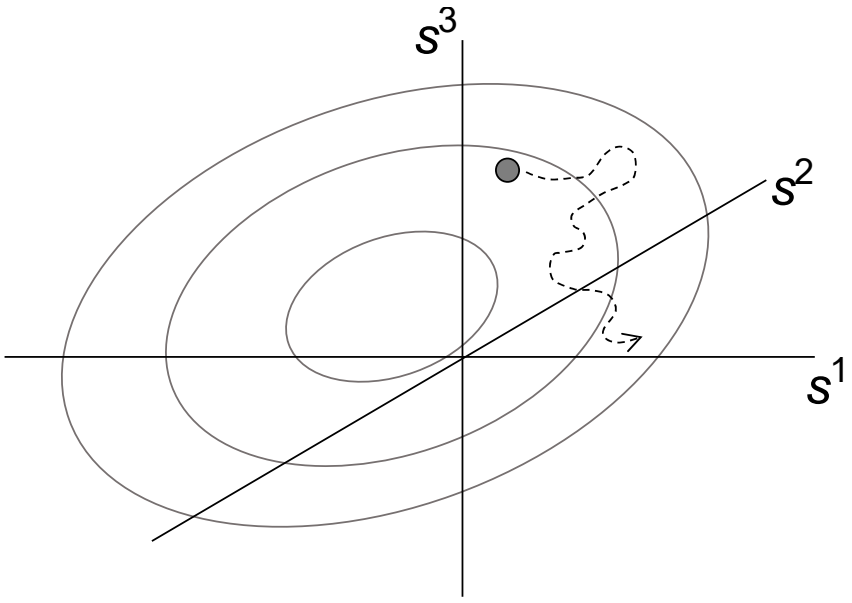

FIG. 1. A gas of model-space shuttles. Points in model space move randomly, but are preferentially attracted to regions of low energy induced by the objective function. The result is akin to an atmosphere of model space points, with higher density and pressure as the minimum of the misfit is approached.

Vectors and tensors in curved space

Kris Innanen

ABSTRACT

Elsewhere in this report we develop the idea of navigating in model space (e.g., to construct the best estimate of an Earth model) not as usual, by being guided by an external objective function and its derivatives, but rather, by following the simplest possible paths in a space that is curved by the objective function. This requires ideas of Riemannian curvature, parallel displacement, and geodesics to be reviewed. This review can be considered as an addendum to the review on tensor analysis in non-Cartesian coordinate systems in the 2020 report.

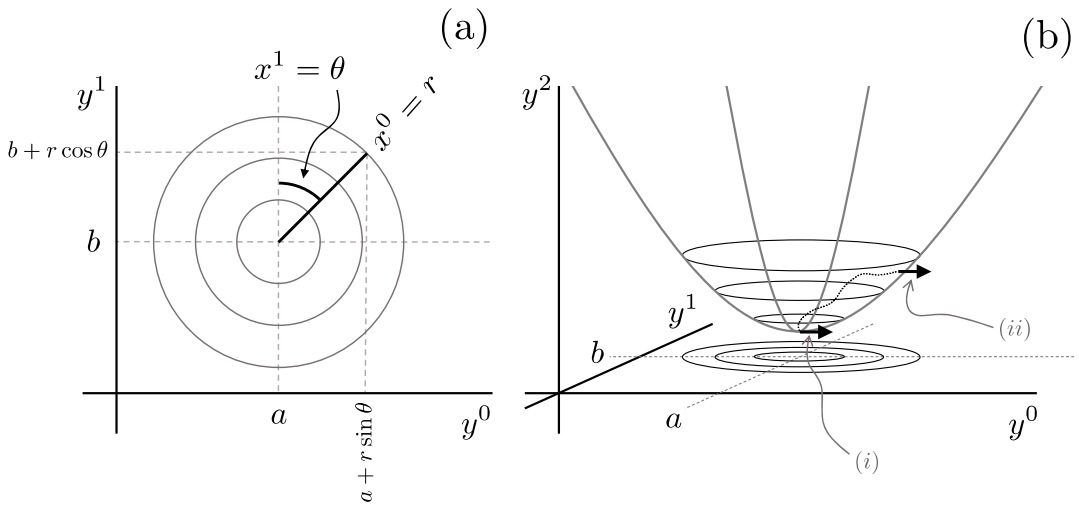

FIG. 1. (a) A 2D space x overlain with a polar coordinate system. (b) The 2D space as a curved surface embedded in a 3D flat space y.

Effective sources: removing the near surface from the VSP FWI problem

Scott Keating*, Matt Eaid, and Kris Innanen

ABSTRACT

For land seismic surveys, the near-surface is often highly variable, resulting in a complex, substantial impact on data. This can make full-waveform inversion very difficult to apply on land seismic data sets, as accurate characterization of the near-surface can be extremely challenging. To cope with this challenge, we propose a full-waveform inversion strategy for removing the near-surface from the inversion problem in the case of vertical seismic profile data. To remove the near-surface from the inversion, we invert for both a subsurface model and a wavefield at a depth below the near-surface. In synthetic examples, we demonstrate that the inversion can accurately characterize the subsurface in this type of approach.

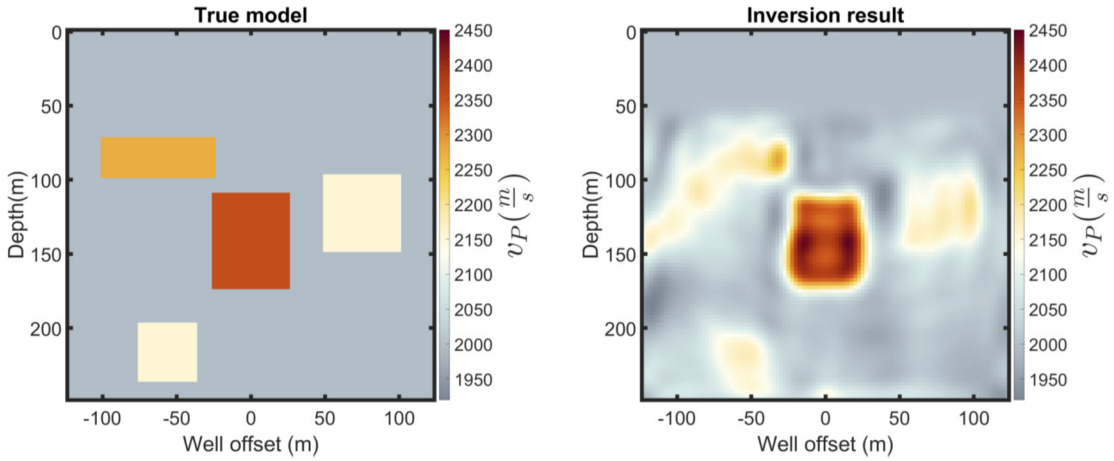

FIG. 1. v_P values of the true (left) and inverted (right) model for a synthetic test. For this test, receivers are present in a vertical column at offset 0 m (representing the well bore), while z-oriented point-forces are deployed in a line at depth 0m. Here, we remove the top 50 m of the subsurface from the inversion problem and instead invert for an effective wavefield at 50 m and the medium below that depth. Overall, the inversion successfully identifies each block, and represents them well in areas with good data coverage.

Full waveform inversion of VSP accelerometer data from the CAMI field site

Scott Keating, Matt Eaid and Kris Innanen

ABSTRACT

The 2018 CaMI VSP survey provided a data-set suitable for creating a baseline subsurface model for later monitoring comparisons. Here, we implement elastic full waveform inversion to obtain an estimate of subsurface properties. Several challenges exist in applying full waveform inversion on the field data, including in particular a complex, difficult to characterize near-surface and discrepancies between geometrical spreading in 2D simulations and field data. We develop approaches for coping with these challenges, and obtain an inversion result that accurately reproduces the measured data. The inversion results in a subsurface model that is plausible, but difficult to verify.

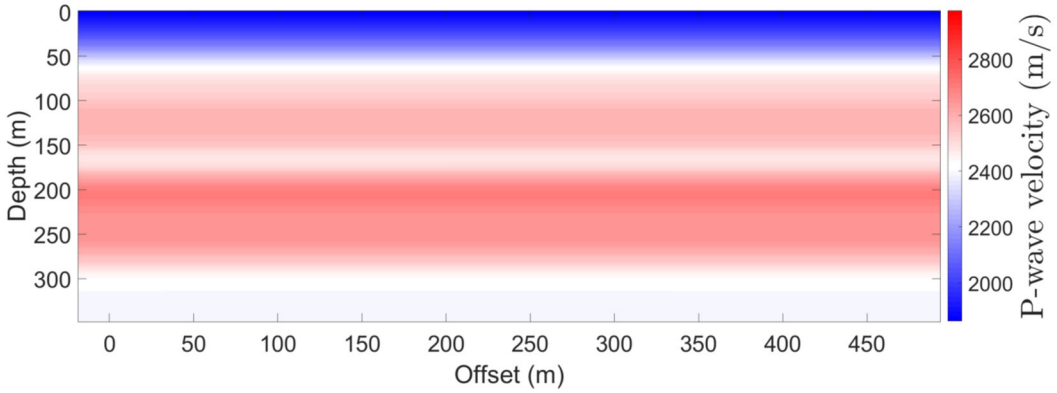

FIG. 1. v_P values of the initial model used.

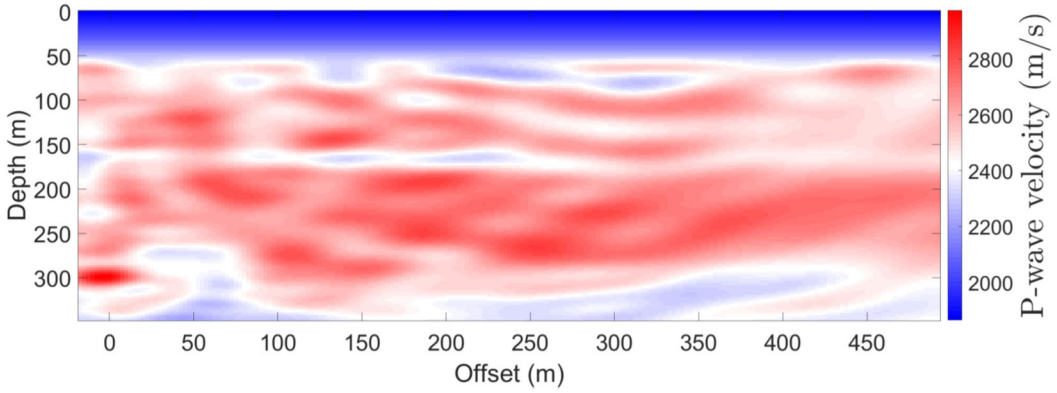

FIG. 2. v_P values for the inversion result. Compare to Figure 1.

Time-lapse analysis of CaMI.FRS CO_2 VSP data

Brendan J. Kolkman-Quinn*[1], Don Lawton[12], and Marie Macquet[2]

ABSTRACT

The Containment and Monitoring Institute Field Research Station (CaMI.FRS) operates a carbon sequestration experiment near Brooks, Alberta. By March 2021, 33 tonnes of CO_2 had been injected into a Basal Belly River Fm sandstone at 300m depth, as a simulation of a shallow leak from a CO_2 storage reservoir. Vertical Seismic Profiles (VSP) were collected between 2017 and 2021 to determine the detection threshold and monitor the plume of injected CO_2. These field data had high repeatability, with permanent borehole geophones and identical shot coordinates, with only surface conditions adding variability. A finite-difference VSP forward model was created to predict the 2D time-lapse response of the CO_2 plume and allow for testing of processing parameters with noiseless data. The 10Hz-150Hz field data required careful processing. A time-lapse compliant processing workflow was developed by paring down a standard VSP workflow, with the goal of avoiding unnecessary alterations to amplitude and phase. This simplified and minimized the cross-equalization between baseline and monitor amplitude spectra: Applying a pre-stack shaping-filter preserved most of the frequency content, at the cost of diminishing the amplitude of the CO_2 time-lapse anomaly. Alternatively, applying custom high-cut filters to the baseline and monitor shot gather pairs reduced the overall frequency content but preserved amplitude contrasts in the reservoir, yielding a higher-confidence result. The 2019-2017 time-lapse difference for a 15t of injection did not unequivocally detect the plume, showing a faint CO_2 anomaly amid background residuals of similar amplitude. The 2021-2017 results showed a higher-amplitude time-lapse anomaly similar to model's predictions. The normalized-root-mean-square (NRMS) difference between reflection amplitudes ranged from 10%-20% in the field data, above the noiseless model's NRMS of 8%-13%. The interpreted CO_2 plume had a 45m-51m lateral extent with an asymmetric distribution around the injection well, indicating greater permeation towards the south-west than to the north-east. A detection threshold between 15t and 33t of CO_2 in a 10% porosity reservoir has been confidently established. These findings will help inform Monitoring, Measurement and Verification (MMV) procedures at future CO_2 sequestration operations.

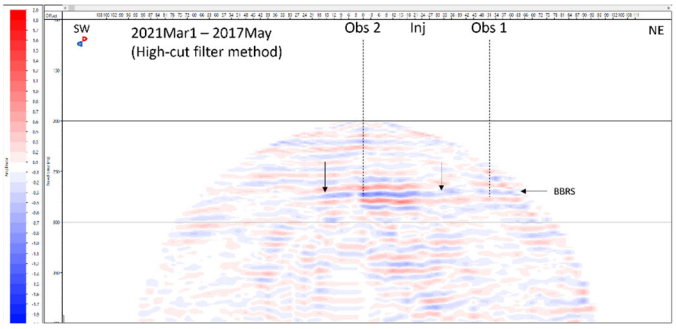

FIG. 1. The 33t CO_2 anomaly was detected and delineated after time-lapse compliant processing.

[1] CREWES, University of Calgary
[2] Carbon Management Canada

Factoring the wave eqn for fast, implicit numerical solutions

Michael P. Lamoureux and R. J. Vestrum

ABSTRACT

Numerical solutions to the wave equations that arise in seismic imaging have been richly developed over the last 70+ years, and typically depend on explicit time-stepping or Fourier techniques for fast, accurate solutions. The counterpart to explicit methods are implicit methods which have enjoy features such as unconditional stability, but typically are computationally prohibitive in two and three spatial dimensions. We demonstrate here a fast, stable implicit time-stepping numerical method for solving the wave equation in two dimensions and higher, that makes use of novel operator factorization in a grid algebra. Several computational demonstrations of the method are presented as well.

This is a summary of the main results described in the MSc thesis of the second author.

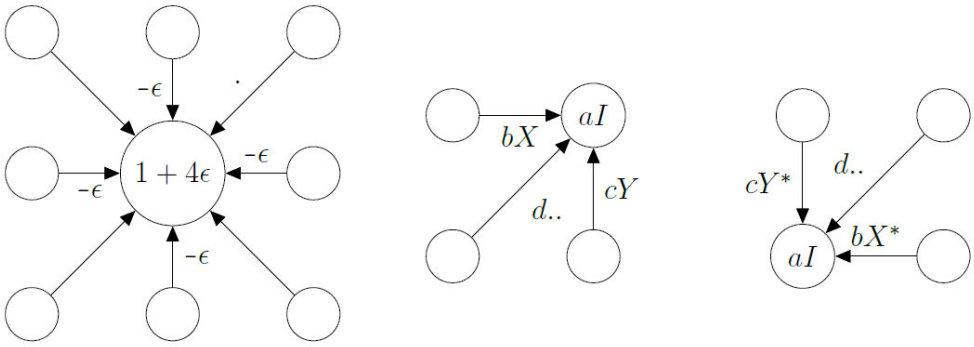

FIG. 1. Shifted 2D Laplacian and its factors $F = aI + bX + cY + dXY$ and F^*, graphically.

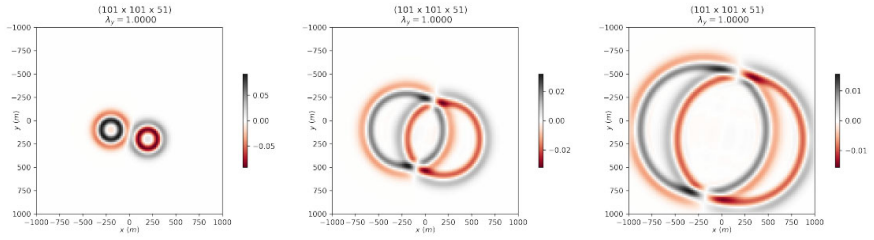

FIG. 2. Sample 3D implicit scheme, two sources, t = 50; 150; 250 msec.

Traveltime tomography: first break picking and machine learning

Bernard K. Law and Daniel Trad

ABSTRACT

One of the most laborious and problematic tasks in refraction tomography is the first arrival traveltime or first break (FB) picking. Many automated FB picking methods determine the arrival time by the difference in amplitude, phase, or frequency characteristics between the data before and after the FB and are often done on a trace-by-trace basis. Spatial correlation between adjacent traces is only used for subsequent editing of mis-picks. The final step in FB picking is to confirm or manually modify the FB picks by trained technicians. With experiences from a large number of datasets with different topography and near-surface geological setting, experienced technicians can recognize the relationship between the FB and the complex waveform of the first arrival energy and various interfering noises. With increasing data density, this has become a very time-consuming and expensive process. In this report, we experiment with two Machine learning approaches: 1) unsupervised automated editing of outlying picks by clustering. 2) supervised deep learning by training the networks with manually edited FB and classifying the first arrival energy waveforms as pre-FB and post-FB. With a catalogue of images of trained models, the deep neural works will be able to classify the first arrival energy waveforms of new datasets as pre-FB and post-FB as accurately as the trained technicians.

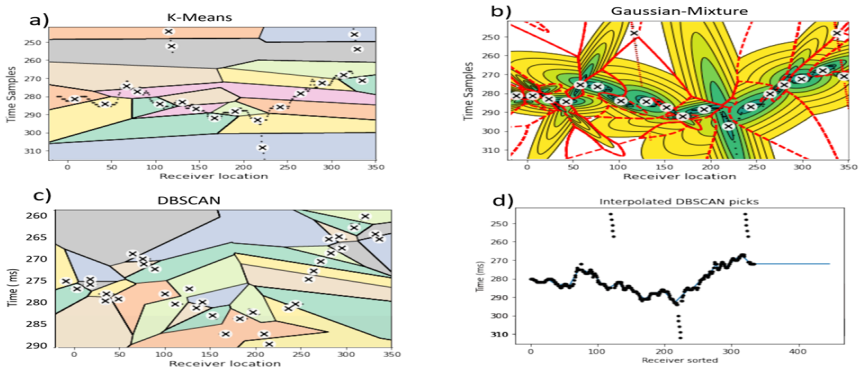

FIG. 1. Different clustering algorithms applied to first break picking.

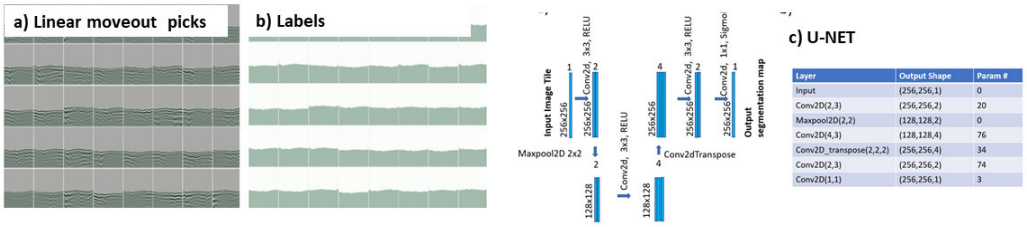

FIG. 2. First break picking by image segmentation using a very simple U-NET.

CO_2 monitoring at the CaMI Field Research Station - update

Don Lawton*[1], Greg Maidment[2], Marie Macquet[2], Al Châtenay[3], Celina Giersz[4], and Amine Ourabah[4]

ABSTRACT

The Containment and Monitoring Institute of Carbon Management Canada collaborates with CREWES on several aspects of monitoring of CO_2 storage at a Field Research Station (CaMI.FRS) in southern Alberta. At this site we are injecting a small amount of CO_2 (several tens of tonnes/year) into the shallow subsurface (300 m depth) to simulate CO_2 leakage from a deeper and larger scale CO_2 storage project. The site provides a field opportunity to test new seismic and other monitoring technologies for monitoring CO_2 storage. In the summer of 2021, an ultra-high-density 3D surface seismic program was recorded at the site in a partnership between Explor, STRYDE and CMC, with CREWES staff also contributing personnel to the acquisition program. The purpose of the acquisition program was to evaluate the viability of using ultra-high-density surface sampling to improve imaging and detection of reservoir characteristics at the site and to aid future designs of 4D time lapse surveys at this and other sites. A total of 19,872 STRYDE nodes were deployed on a 7.5 x 7.5 m grid over an area of 1 km x 1 km into which 9,041 shots were recorded using a new proprietary seismic Explor source (PinPoint). In addition to 3,910 records obtained using the University of Calgary Envirovibe source, making this arguably the highest trace density of a land 3D survey ever recorded. The processing of the data is continuing, the main processing challenge being generally a high level of noise observed in data. However, initial results are very promising, as shown in the Figure 1 which shows an in-line from the 3D volume of PinPoint data compared to an equivalent in-line from the baseline survey from 2014.

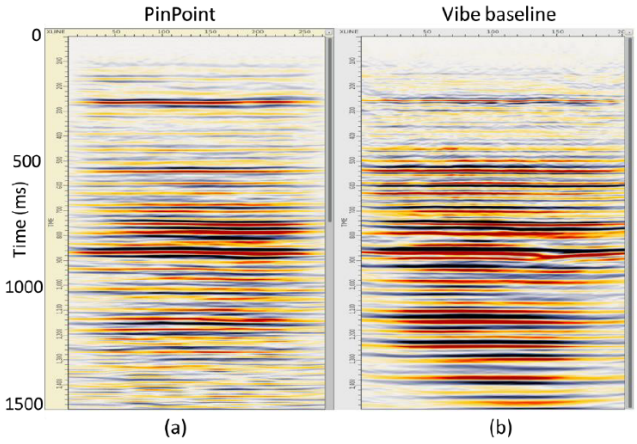

FIG. 1. Comparison of initial processing of (a) PinPoint data (one pass of denoise and post-stack time migration) with (b) legacy vibe data (post-stack time migration).

[1] University of Calgary
[2] Carbon Management Canada
[3] Explor
[4] STRYDE

A review of seismic-while-drilling technique: from 1986 to 2020

Jinji Li and Kris Innanen

ABSTRACT

Seismic-while-drilling (SWD) is a technique that explicitly creates an array of sources together with the progression of drill bit towards deeper layers. It provides great potential in energy industries, and surveying geophone arrays can receive the signals from underground, thus providing additional information. In the past few decades (1986-2020), the industry and researchers systematically realized many advantages of SWD and made it a merging project. SWD is often acknowledged as a promising auxiliary tool in exploration geophysics since the additional ray paths generated from the subsurface can complement current seismic exploration approaches, which need a relatively comprehensive acquisition. For example, Full-Waveform-Inversion and migration. However, this technique still needs to be further exploited before being widely utilized. This paper aims to summarize the basic principles of SWD and review the progress, mainly focusing on its practical applications in exploration seismic from the 1980s to recent for supporting future development directions.

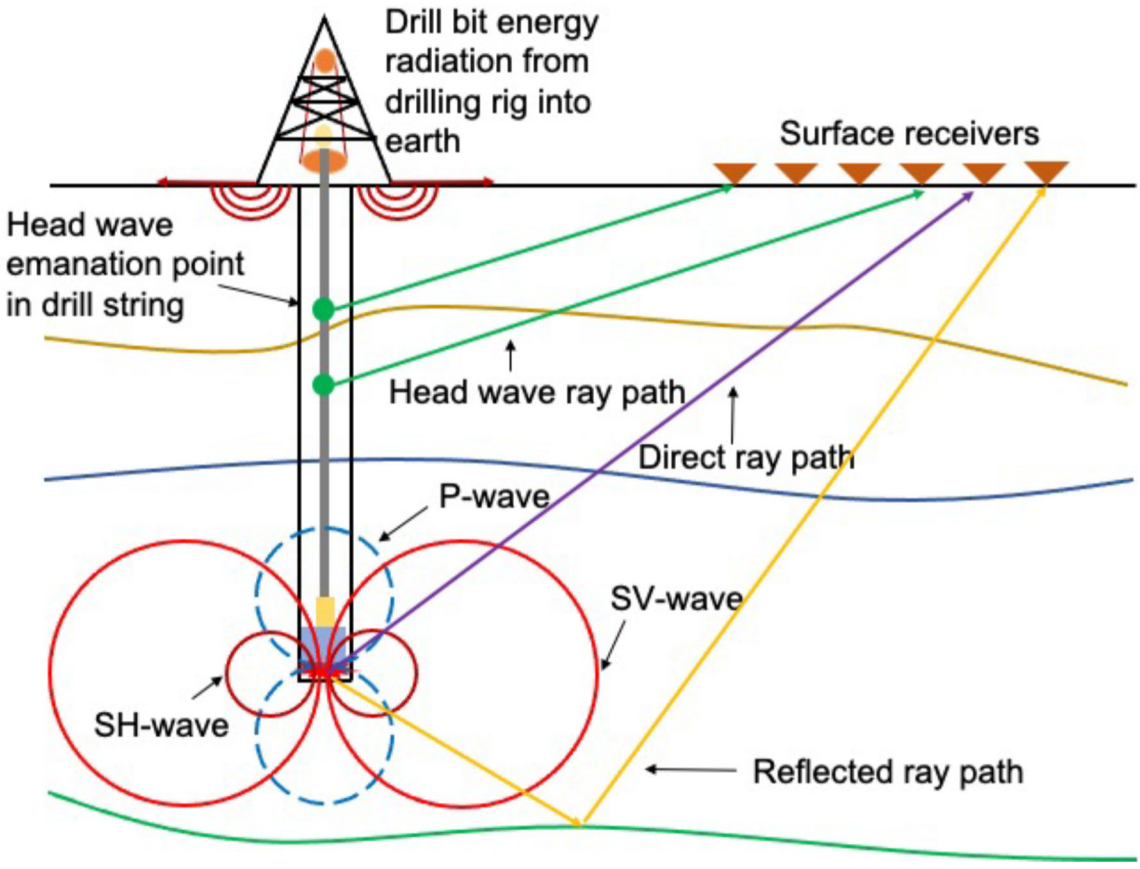

FIG. 1. Seismic-while-drilling radiation patterns in the vertical well.

Simultaneous waveform inversion for velocity, density and source moments with application to seismic-while-drilling

Jinji Li*, Scott Keating, Roman Shor, and Kris Innanen

ABSTRACT

Full waveform inversion (FWI) is an optimization-based approach to estimating the subsurface parameter model that minimizes the difference between synthetic and real data iteratively. In practice, incomplete acquisition and illumination of the subsurface are strong limiting factors. Adding data corresponding to new and independent ray paths as input could lead to significant increases in the reliability of FWI models. In principle, seismicwhile-drilling (SWD) can supply these additional ray paths but introduce a new suite of unknowns, namely precise source locations and radiation characteristics. Here we formulate a new elastic FWI algorithm in which source positions and radiation patterns join the velocity/density values of the grid cells as unknowns to be determined. We then carry out a synthetic feasibility study in which such incompletely-known sources are included along a plausible well-trajectory through a simulated model, around which seismic receivers are placed in various configurations. This SWD-FWI is optimized with a Truncated Gauss-Newton algorithm. The subsurface model and source properties (P-wave velocity, density, and three independent 2D moment tensor values) are recovered and analyzed. The analysis suggests that the participation of SWD improves the accuracy of FWI models, especially in density inversion. The inversion of elastic properties shows a similar improvement when different drilling paths participate, which is different than expected. Such results indicate further related study is required to provide more comprehensive radiation patterns of the SWD sources.

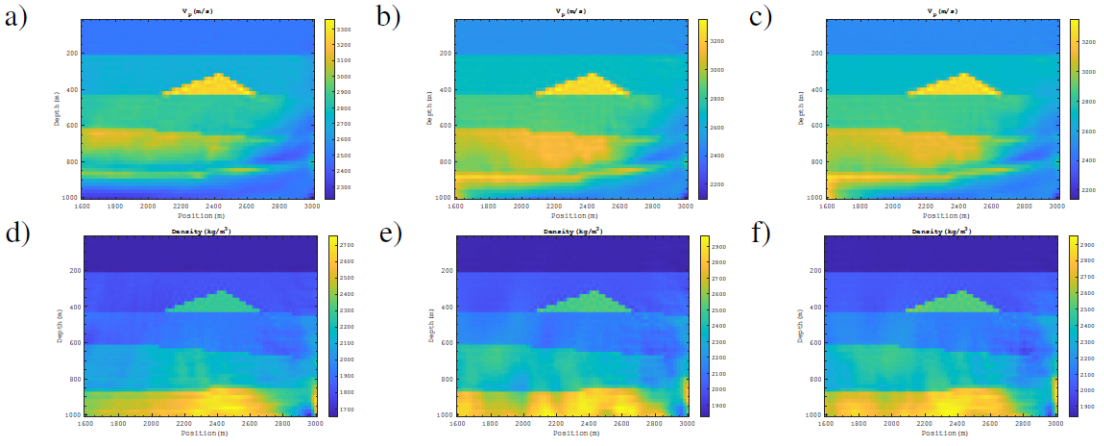

FIG. 1. Inversion result of subsurface properties. a) Compressional velocity, b) Density, c) Compressional velocity (vertical drilling path added), d) Density (vertical drilling path added), e) Compressional velocity (deviate drilling path added), f) Compressional velocity (deviate drilling path added).

Amplitude-encoding FWI using different bases

He. Liu*, Daniel Trad, and Kris Innanen

ABSTRACT

A super-shot or blended data strategy has been used in marine and land seismic surveys to reduce acquisition costs by reducing the time spent on the field. Full waveform inversion (FWI) has been used to estimate high-resolution subsurface velocity models. However, it suffers from expensive computational costs for matching the synthetic and the observed data. To reduce the costs of both data acquisition and processing, FWI using blended data has been recognized as very promising in future oil exploration. In this work, we use an amplitude-encoding strategy with different bases to accelerate the FWI process and compare their performance. The synthetic examples show that amplitude-encoding FWI using different bases as encoding functions can mitigate the crosstalk noise very well, providing good estimations of velocity models and convergence rate for both acoustic and elastic media. To further improve the calculation efficiency, we also adopt the dynamic encoding concept and reduce the number of super-shots every a few iterations. Since the encoding functions are not changed during the iterations, we can directly simulate the super-shots without the blending stage. From the updated velocity model comparison, we can see that the inversion results by dynamic encoding are almost identical to those by static encoding with further reduced calculation effort.

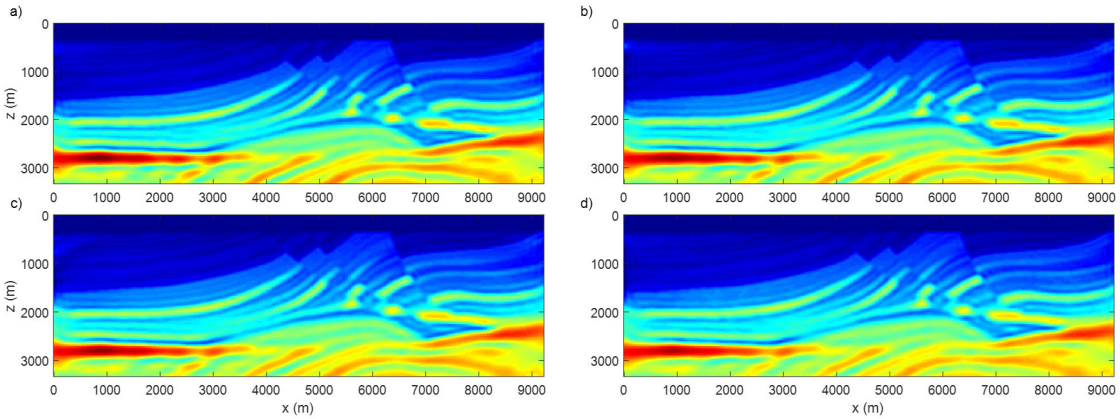

Fig. 1. Inversions results using dynamic-encoding concept by different bases: a) Hartley; b) cosine; c) sine and d) random polarity.

Insights on Domain Adaptation for fault identification

Mariana Lume, Marcelo Guarido, David Emery, and Kris Innanen

ABSTRACT

Conventional deep learning has proved to be successful for fault identification tasks if the dataset selected for training and testing a model belong to the same domain. When it does not occur, the classifier usually degrades its performance. This study focuses on explaining the successes and failures of applying a model, previously trained with synthetic seismic images, on two different datasets of synthetic and real seismic images. When considering synthetic datasets, the classifier was very accurate; however, in the second scenario, a significant number of misinterpreted faults appeared. These outcomes are a direct consequence of the similitudes or discrepancies between both datasets used, hence Domain Adaptation techniques are usually applied to overcome the encountered challenges.

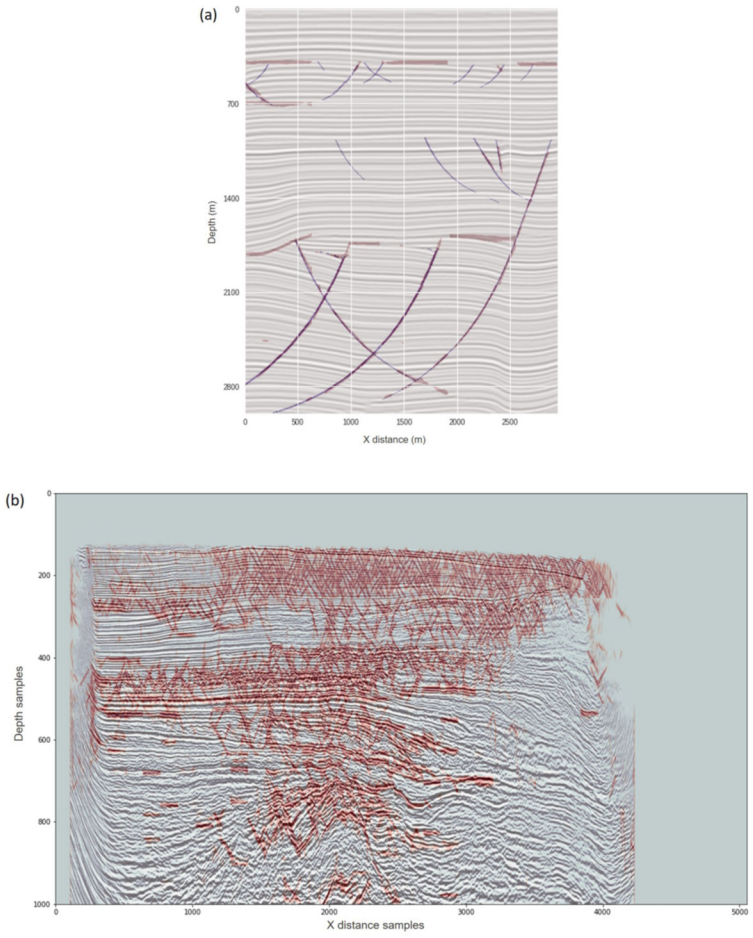

FIG. 1. Predicted faults (red color) after applying conventional DNN: (a) The model trained with synthetic data and was tested on a different synthetic dataset. (b) The model trained with synthetic data and was tested on real seismic images of a different geologic area.

Local optimization approaches for simultaneous AVO inversion based on re-parameterized Zoeppritz equations

Mariana Lume* and Kris Innanen

ABSTRACT

Linearized AVO inversion methods, such as the weighted stacking approach, are based on approximations of the Zoeppritz equations subject to several assumptions, including the limitation of incidence angles to 35-40°, typically smaller than the critical one. Thus, in long-offset acquisitions these approaches fail. This study focuses on developing a nonlinear inversion appropriate under these circumstances, based on re-parameterized Zoeppritz equations in terms of the fractional density and compressional and shear impedances. To achieve this, P-P and P-S datasets with different characteristics of noise and frequency are considered. In general, conditioned to a good initial model, three different local optimization algorithms demonstrate a superior performance respect to the simultaneous weighted stacking inversion, producing more accurate results for most elastic parameters, and the inclusion of noise information during the inversion improves the fractional shear impedance and the fractional Vp/Vs ratio, promising a better rock properties estimation.

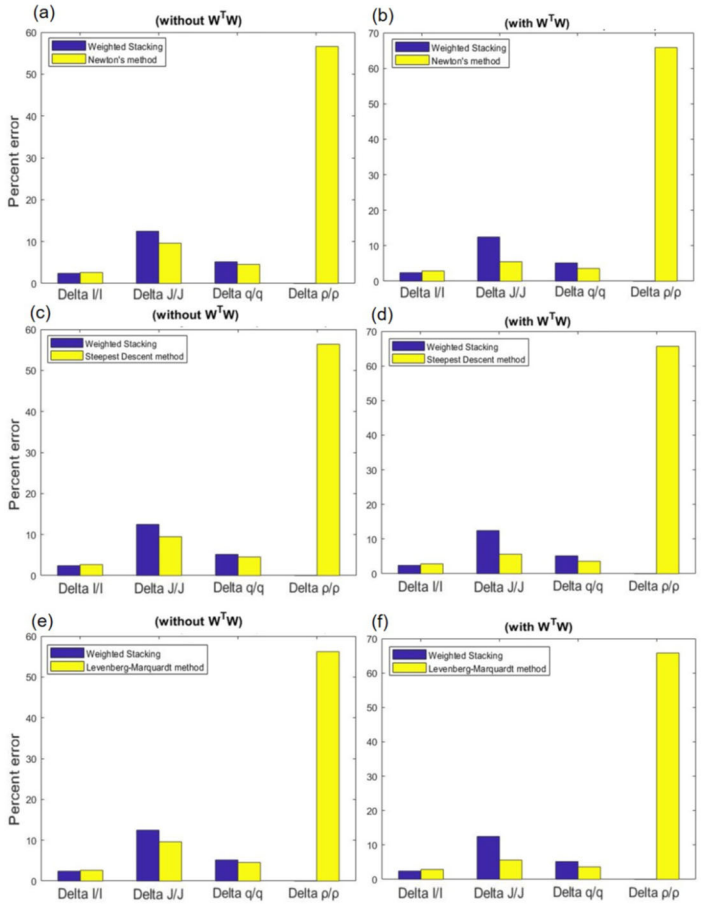

FIG. 1. Nonlinear and linearized inversion results after using band-limited and noisy reflectivities, as well as noise information ($\mathbf{W}^T\mathbf{W}$).

An encoder-decoder CNN for DAS-to-geophone transformation

Jorge E. Monsegny*[1], Daniel Trad[1], and Don Lawton[12]

ABSTRACT

Distributed acoustic sensing is a technology that uses optical fibre to record seismic waves. While traditional geophones record the particle velocity created by a passing wave, optical fibre records the strain or strain rate. The conversion between the two kind of signals allows seismic time lapse imaging applications with data from these two different recording systems. Here we use convolutional neural networks to transform fibre to geophone data. Instead of using a supervised model where we provide examples of corresponding fibre and geophone traces, we utilize an encoder decoder scheme that receives fibre traces and produces fibre traces. The important distinction is that the decoder is deterministic and contains the physics of transforming a geophone trace to a fibre trace while the encoder is the convolutional neural network that does the opposite transformation. The whole encoderdecoder is trained to be the identity operator on fibre traces. At the end of the training, the application of the encoder part alone will perform the desired signal conversion from fibre to geophone.

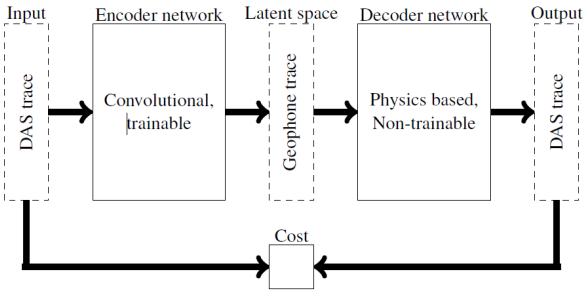

FIG. 1. DAS to geophone encoder-decoder neural network. The input and output is the DAS trace and the whole network acts like an identity operator. The encoder part is a CNN that transforms DAS to geophone, the latent space. The decoder part is non trainable and physics based that transforms geophone to DAS.

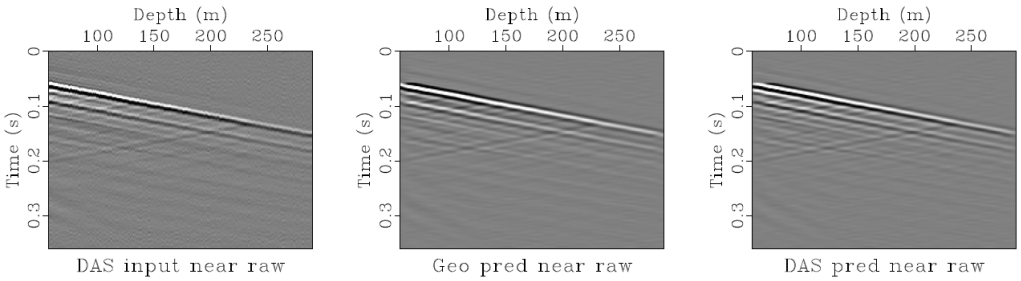

FIG. 2. Left column are the input DAS gathers, the middle column contains the predicted geophonegathers (in the latent space), and the right column are the predicted DAS gathers.

[1] CREWES, University of Calgary
[2] Carbon Management Canada

Passive source location by diffraction scanning

Jorge E. Monsegny*[1], Don Lawton[12], and Daniel Trad[1]

ABSTRACT

During CO_2 injection monitoring several events generated by passive sources at different locations are recorded. Some events are from surface operations while others are consequence of the CO_2 injection. We use a technique that analyzes the moveout of the passive seismic events for a series of potential sources located at different positions in the subsurface. The technique generates a plot that catalogs the events by source location making possible to discern events produced the zone of interest from events generated elsewhere. We apply the technique to passive seismic records at the Containment and Monitoring Field Research Station in Alberta, Canada.

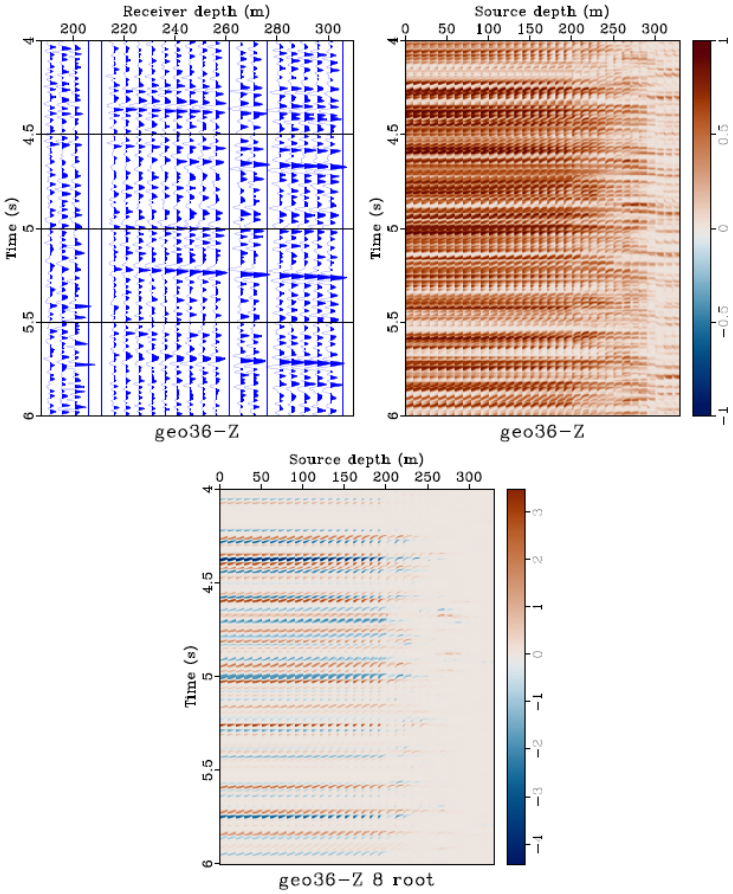

FIG. 1. Passive seismic record and moveout plots for semblance, above, and 8-th root staking, below. The plots show that most of the events are generated by sources located above the seismic array, probably at the surface. Some anomalies are located in the geophone array zone below 200m.

[1] CREWES, University of Calgary
[2] Carbon Management Canada

Reducing the influence of coherent noise on FWI with misfit modification

Luping Qu*, Xin Fu, and Kris Innanen

ABSTRACT

As field data applications of FWI increase in number and ambition, dealing with the presence of both random and coherent noise in seismic data, and the artifacts they create in FWI models, becomes increasingly important. Though noise suppression methods, including various filters and decompositions, applied before the inversion, can mitigate these to some extent, remnant noise still always exists in the processed data. In this study, we carried out a systematic study of the impact of noise on scalar acoustic FWI models and sought mitigation strategies. We found that while random noise with low SNR (<=20%) does not exert a strong influence, correlated noise of all types tends to produce a strong negative affect. Mitigation effort here is likely to pay dividends in model accuracy and reliability. We examine the effect of including the data covariance matrix into the misfit function. Through iterative processing, random and correlated noise, and their combination, can be estimated during FWI. As limited frequency bands contribute most of the signal, high frequency bands (>=35 Hz) were cut off. Considering accuracy and computational efficiency, the data can be resampled every two or three points in the frequency domain. The intermediate results of misfit and gradient were calculated by individual frequency and then transformed back to time domain after interpolation. The misfits are then calculated by individual frequency and transformed back to the time domain after interpolation. Numerical testing is suggestive that this approach improves on more conventional de-noising methods.

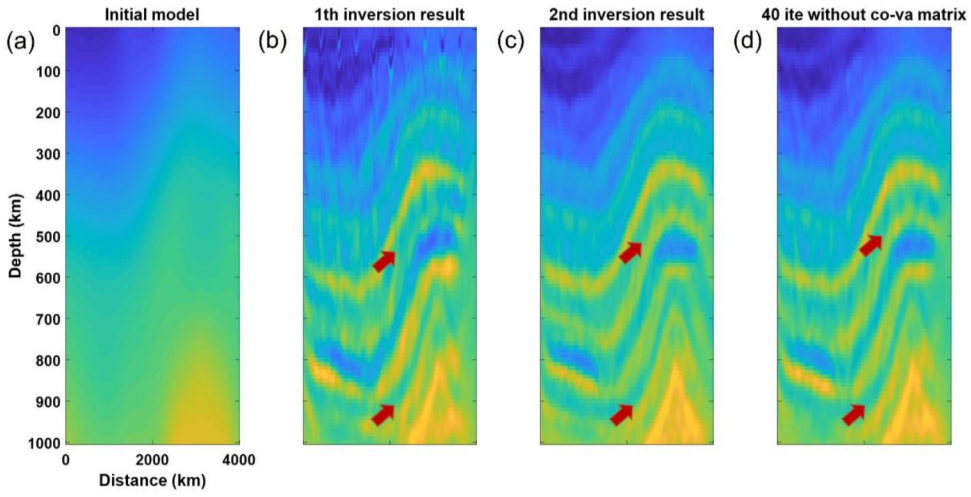

FIG. 1. Inversion results. (a) Initial model, (b) the inversion result of the conventional FWI after 20 iterations, (c) the inversion result of the modified FWI after 20 iterations, (d) the inversion result of the conventional FWI after 40 iterations.

Reducing the influence of remnant noises on elastic FWI with misfit modification

Luping Qu, Scott Keating, and Kris Innanen

ABSTRACT

Seismic data collected in the field are mostly elastic data including body waves, surface waves, and unwanted noises from various sources. Compared with acoustic FWI, noise suppression or estimation in a elastic engine are of more practical significance. Various types of noise may exert different influences on the multi-parameter estimation in elastic FWI. In this study, we analyzed the influence of random and correlated noises on the estimation of model parameters V p, V s, and density. To mitigate the influence of the noises, we adopted the modified FWI misfit, in which the data covariance matrix is incorporated, to invert the elastic model parameters while estimating the noises in seismic data. The data covariance matrices calculated from the data residuals, which were obtained from a first round of FWI, were generated and applied in the following iterative inversion. As the elastic FWI was conducted in the frequency domain, the dimension size of the data covariance matrix is calculated by each frequency, and it is not likely to cause the out-of-memory problem. Two types of noises including random noises and correlated noises were added to the true spectra and estimated in the modified FWI. The inversion results were compared with the results of the conventional FWI with the same iteration number.

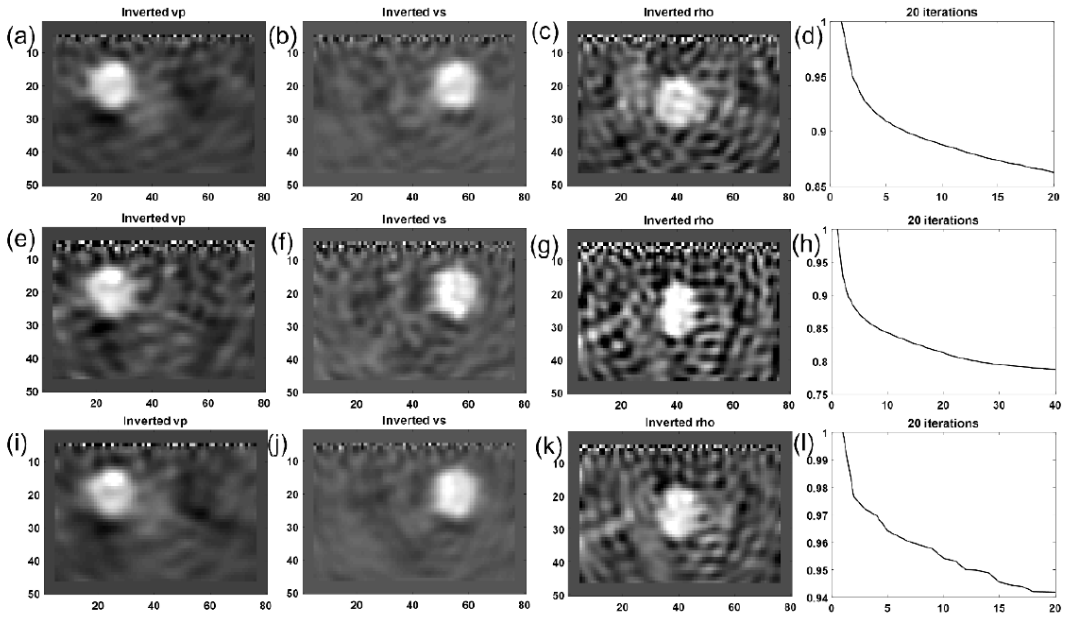

FIG. 1. Inversion results. (a) Inverted Vp model of the first FWI, (b) Inverted Vs model of the first FWI, (c) Inverted density model of the first model, (d) the misfit change of the first FWI, (e) inverted Vp model of the conventional FWI using 40 iterations, (f) inverted Vs model of the conventional FWI using 40 iterations, (g) inverted density model of the conventional FWI using 40 iterations, (h) the misfit change of the conventional FWI with 40 iterations, (i) inverted Vp model of the second FWI with the modified misfit, (j) inverted Vs model of the second FWI with the modified misfit, (k) inverted density model of the second FWI with the modified misfit, (l) the misfit change of the second FWI with modified misfit.

Seismic facies classification with parametric and nonparametric statistics

Brian Russell*[1]

ABSTRACT

In this presentation, I first compare parametric and nonparametric statistical methods for seismic facies classification using a simple example that involves two seismic attributes, two facies and ten points. I will then move to a real data example, in which seismic facies classification is used to identify by-passed oil in a North Sea field.

Before applying statistical methods of classification to the ten-point problem, I first applied two simpler methods: least-squares and k-nearest neighbor, or kNN, classification. I then moved to statistical classification using two different approaches: Bayesian classification using the bivariate normal Gaussian distribution and kernel density estimation (KDE) using a Gaussian kernel. Bayesian classification with the normal distribution is called a parametric statistical approach since it uses a limited set of parameters to perform the classification (i.e., the mean, variance, and covariance of each class). KDE is similar except that it applies a Gaussian distribution to each point in the two classes and sums the result. Although KDE is dependent on the width of a scaling parameter, it is called a non-parametric statistical method because it is dependent on all the points in each class. Finally, I show how a deep feedforward neural network (DFNN) can be used to solve the same ten-point classification problem.

In summary, it was found that least-squares did a very poor job of separating the classes and, although kNN did an excellent job, it did so by using linear segments rather than a smooth boundary. The Bayesian parametric approach gave a smooth boundary but miss-classified some of the points, whereas the KDE and DFNN approaches both gave smooth boundaries and were both able to perfectly classify the points in each facies. However, since the DFNN approach is highly dependent on the structure of the network and is also time consuming to run, the KDE approach was chosen as the optimum method to apply to the real data example.

In the North Sea example, five classes were first derived from the four well logs in the area and then a cross-plot of VP/VS ratio versus P-impedance was used to predict these classes from the seismic inversion results. This involved first building rock physics models for each of the five classes and then using Monte Carlo simulation to create many simulated values. The simulated values were then used to train the KDE classification technique. Finally, the trained KDE algorithm was applied to the cross-plot of VP/VS ratio versus P-impedance from the inverted seismic volume to predict the classes over the volume. The result showed an area of by-passed oil on the survey, between two of the wells.

[1] CGG GeoSoftware

Shiny web applications for unsupervised learning optimization applied to diagnostic fracture injection test event detection

Lukas Sadownyk*, Marcelo Guarido, Danial Zeinabady, Erfan Sarvaramini, Zhenzihao Zhang, Farshad Tabasinejad, Hashem Salari, Kris Innanen, and Christopher R. Clarkson

ABSTRACT

Diagnostic Fracture Injection Tests (DFIT), are commonly used to derive key parameters and other parameters for hydraulic fracture design and modeling. Although this process can identify properties needed for well optimization, it is also time intensive and affected by human interpretation bias. In this report, we address this adversity by applying unsupervised clustering methods: K-Means, DB-Scan, Hierarchical modeling, and Gaussian mixture models to identify point density variation that correlates to key parameters on a DFIT curve. A R-Studio Shiny Web App is developed to apply these methods and provide a user-friendly platform for adjusting input variables and hyperparameters. Exploring the clustering approach emphasizes the importance of different variable combinations as well as noise considerations when interpreting a DFIT curve with clustering methods. Principle Component Analysis (PCA) further demonstrates why clusters occur where they do along a DFIT curve. Unsupervised clustering applied to DFIT data achieves an unbiased and quick work-flow for event identification that can be scalable to large datasets.

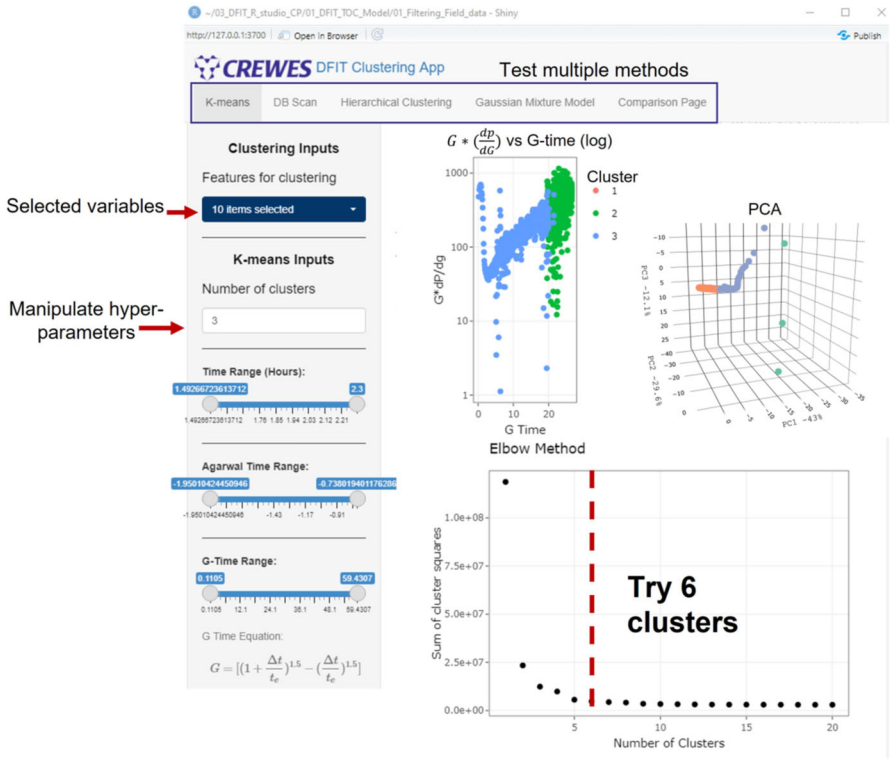

FIG. 1. Screen capture of the interactive CREWES DFIT Clustering App with its various analyticalfeatures highlighted.

Deblending in various domains

Ziguang Su and Daniel Trad

ABSTRACT

Seismic acquisition is a trade-off between economy and quality.Deblending of simultaneous-source data, which allows a temporal overlap between shot records, has significant advantages to improve data quality (e.g., denser shooting) and reduce acquisition cost (e.g., efficient wide-azimuth shooting). Deblending may use the coherency property of the simultaneous-source data that varies in different domains. The common shot gather(CSG) can be converted into common midpoint gather, common receiver gathers, for deblending. Common-image gathers are an important output of prestack depth migration. They not only can provide a velocity model for depth migration, but also can provide amplitude and phase information for subsequent subsurface attribute interpretation. This report investigates the blended data in the common image domain and creates an angle-related deblending method in angle domain common image gather(ADCIG).

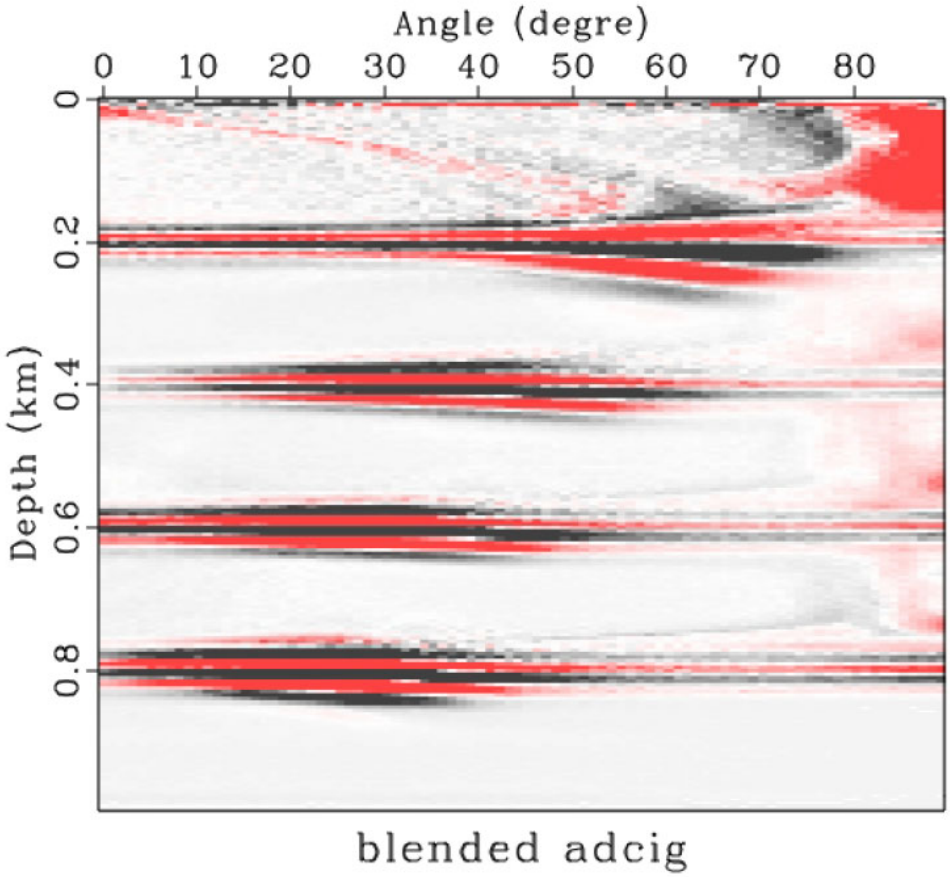

FIG. 1. ADCIG for blended data.

GPU applications for modelling, RTM, FWI and Machine Learning

Daniel Trad*

ABSTRACT

Finite difference (FD) modelling is a key operation in seismic research. We need FD for creating synthetic data and predictions in inversion algorithms, like reverse time migration (least-squares or standard) and full waveform inversion. Supervised machine learning techniques require large databases of synthetic data and labels for training. In this report, we look at the implementation of finite differences using Graphics Processing Units (GPUs) and compare computing times for implementations of all these seismic operations with times achieved by Central Processing Units (CPUs) parallelization in clusters and multithreaded units. Not only do we observe speedups between 30-100x for modelling, RTM and FWI but also we notice that for GPUs the computing time does not increase linearly with the number of operations as it does for CPUs but at a much lower rate. We observe this superlinear scaling phenomenon for increasing order, increasing complexity, and increasing grid size, or equivalently decreasing cell size. This last observation brings advantages for time-domain multigrid FWI, where inversion is solved iteratively on stages of increasing frequency.

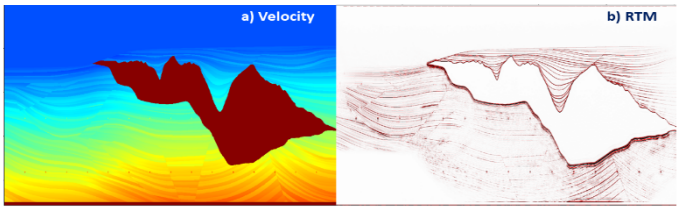

FIG. 1. GPU-RTM for 50 shots with frequency bandwidth between 0-25Hz. a) Initial model, b) RTM. Running time 20 minutes on a desktop with 1 GPU, 60 minutes in a 10 nodes cluster.

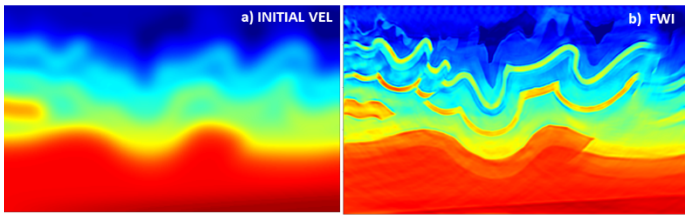

FIG. 2. Multigrid FWI for 50 shots with bandwidth between 0-25Hz. a) Initial model, b) Inverted model with multigrid FWI in 3 stages (32m cell, max Hz, 16m cell, 16Hz, 8m cell, 25Hz).

stage	time expected	time real	ratio expected	ratio real
1	–	206	–	–
2	824	327	4	1.6
3	5100	1466	26	3.6

Table 1 GPU-Superlinear scaling for multigrid FWI. Expected vs Real-time increase when increasing frequency across stages with respect to 1st stage. Times are in secs, stages are 32m->8Hz, 16m->16Hz, 8m->25Hz.

Attenuation estimation from DAS VSP data of CaMI Field Research Station

Yichuan Wang and Don Lawton

ABSTRACT

For seismic monitoring injected CO_2 during geologic CO_2 sequestration, it is useful to measure seismic attenuation. Seismic attenuation directly connects to different petrophysical parameters of reservoir rock or CO_2 capture and storage site. We have used an approach for measuring attenuation by iteratively identifying a sparse set of the strongest reflections in the seismic trace and stacking their waveforms. This method is straightforward and requires no sophisticated inverse algorithm. It is data-driven and shows a trade-off between resolution and estimation accuracy. This method is applied to the DAS VSP dataset from the CaMI Field Research Station (FRS) in Newell County, Alberta. High-quality cross-sections of the differential attenuation parameter 1/Q and its "geometric" counterpart γ are obtained. Strong attenuation of large positive 1/Q or large negative γ around the CO_2 injection well within the CO_2 injection zone of Basal Belly River Sandstone Formation is observed, which is interpreted as being related to the injected CO_2 at the CaMI FRS. The attenuation measured through this approach could be reliable CO_2 indicator.

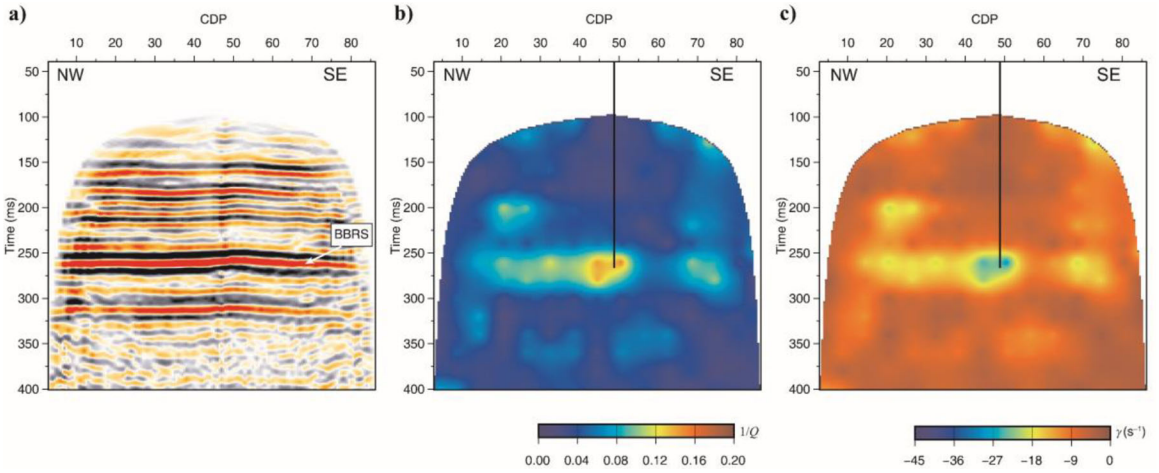

FIG. 1. Attenuation-parameter cross-sections: a) VSP CDP stack from a walk-away line; b) estimated 1/Q values, and c) estimated γ values. The Basal Belly River Sandstone (BBRS) reflection is indicated in plot a). Black line in b) or c) indicates the location and depth of the CO_2 injection well at the CaMI FRS.

Acquiring physically-modeled seismic data using 70kHz piezoelectric buzzers

Joe Wong, Kevin Bertram, and Kris Innanen

ABSTRACT

Efficient full-waveform inversion (FWI) seismic imaging of complex velocity structures requires low dominant frequencies in the range 4Hz to 10Hz. When immersed in water in the laboratory, piezoelectric buzzers such as the one shown on Figure 1 will generate and detect vibrations with laboratory frequencies ranging from 40kHz to 100kHz. Physically-modelled transmission seismograms recorded with buzzer transducers have the low frequencies (after scaling down by a factor of 10^4) required for efficient FWI, but their coda are too long and too variable for them to be ideal FWT source wavelets. Finding ways to mitigate these two unfavourable characteristics is an ongoing task in our research in physical modelling.

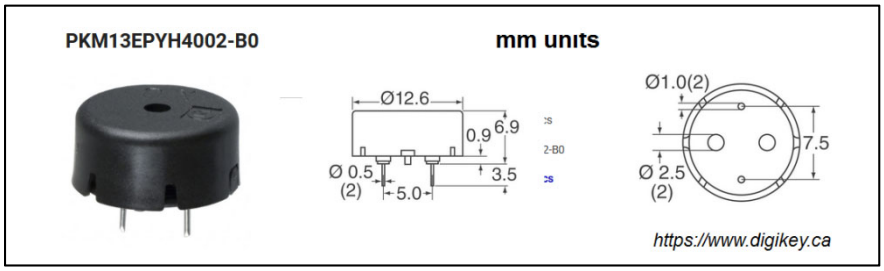

FIG. 1. Piezoelectric buzzer used as sources and receivers in seismic physically modelling.

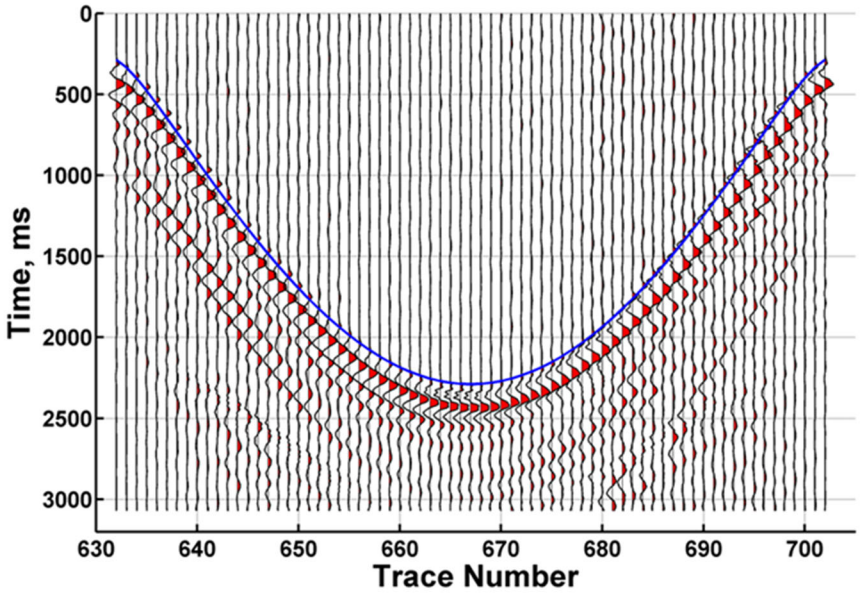

FIG. 2. Trace-normalized display of an example common-source gather of physically-modelled seismograms through a 2D plane in a homogeneous medium (water). Blue line marks calculated water arrival times. The long-duration non-uniform coda and lack of symmetry with respect to the apex position make the traces unsuitable for use in FWI.

Analyzing buzzer-acquired physically-modelled data for FWI

Joe Wong, David C. Henley, and Kris Innanen

ABSTRACT

Physically-modelled transmission seismograms were acquired with piezoelectric buzzers transducers as source and receiver immersed in a homogeneous volume of water. They exhibited laboratory dominant frequencies in the range 40kHz to 100kHz that scal e down to seismic frequencies in the range 4Hz to 10Hz. The scaled frequencies are suitable for efficient full waveform inversion (FWI) in the seismic exploration world. However, the time durations of the observed source/receiver wavelets are very long, and their coda are different for every source-receiver combination. Both factors cause the buzzer-acquired data to be ill-suited for efficient FWI seismic imaging. We applied a time-domain filtering technique to shorten the time durations of the observed wavelets and increase the uniformity of their coda. Figure 1 shows that the time-domain filtering technique worked very well for some traces (e.g., traces near the left and right edges of the display; 10 traces on either side of Trace Number 667), but failed for others. The common feature of traces that converted poorly seems to be the presence of discernible amplitudes past about 700ms. We are hopeful that modifications to the filtering technique can be found that to improve the performance for those traces.

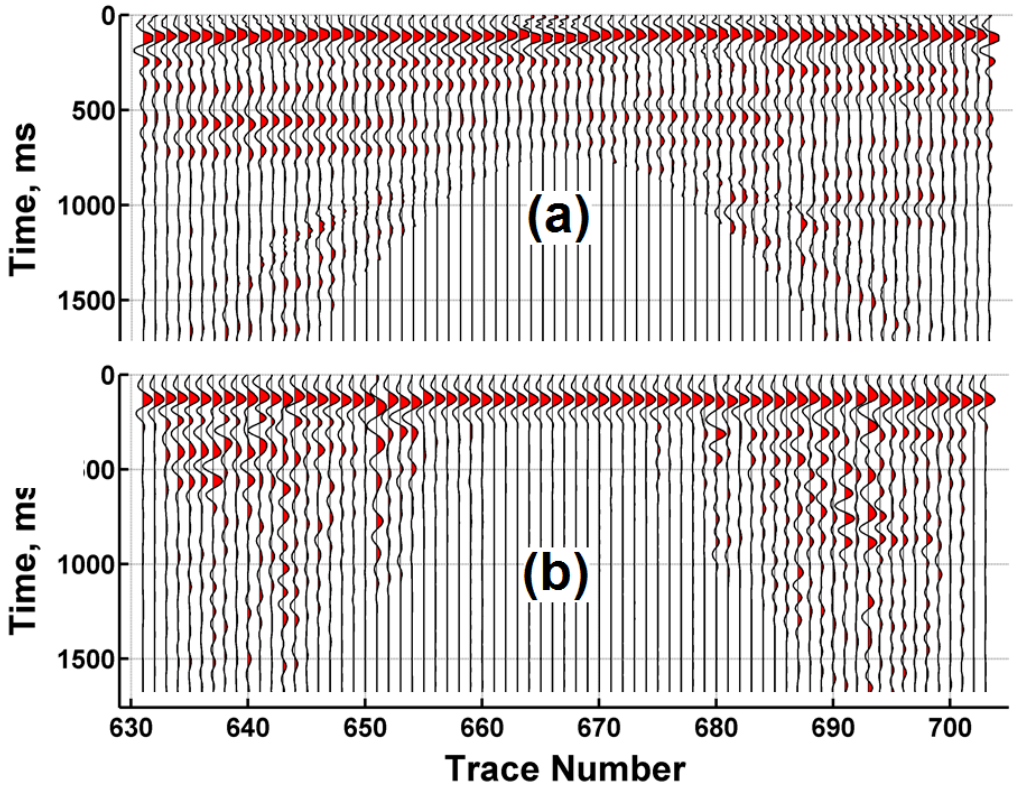

FIG. 1. A time-domain filtering technique is used to convert long-duration, non-stationary signals to short-duration, more uniform wavelets: (a) Input signals. (b) Output signals. Present results show promise but are mixed. The method needs to be modified to improve its performance for input traces that do not convert well.

The implicit neural representation for full waveform inversion

Tianze Zhang*, Jian Sun, Daniel Trad, and Kris Innanen

ABSTRACT

In this study, we introduce the implicit full waveform inversion (IFWI), which uses the neural network to generate velocity models and perform the full waveform inversion (FWI). The IFWI consists of two parts, which are a neural network that generates the velocity models and a recurrent neural network FWI (RNNFWI) to perform the inversion. IFWI has two main features that distinct from the FWI. First, it does not need an initial model like the conventional FWI. IFWI only needs general information about the target area, for instance, the mean and the standard deviation of the physical parameter in the target area, for instance, the well-log information of the target area. Second, in IFWI, we update the weights in the neural network, unlike in the conventional FWI, which updates the velocity model directly. The neural network we use to generate velocity models is a fully connected layer with sinusoidal activation layers. Such a network outperforms a fully connected network with other activation layers, like the Relu and tanh. It is because it has the ability to learn high-order space derivatives. Through numerical tests, we demonstrate that, with the proper control of the random initialization of the weights in the network and the scale of the velocity the network generated, the IFWI can perform waveform inversion without an initial model. We can also use the results of IFWI to provide a good initial model for the conventional FWI.

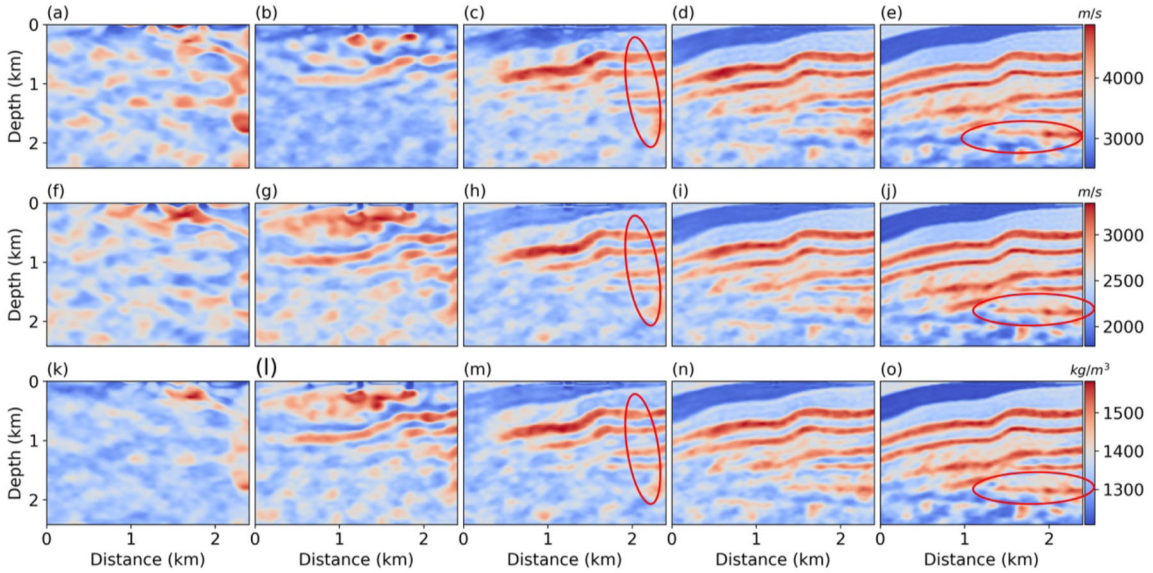

FIG. 1. Elastic IFW inversion results with surface and well acquisition. Figure (a)-(e) shows the inversion results of the VP model at 60, 100, 200, 500 and 2000 epochs. The second and the third row shows the inversion results for VS and density.

Learning elastic wave equation with Fourier Neural Operators

Tianze Zhang*, Kris Innanen, and Daniel Trad

ABSTRACT

In this study, we use the Fourier Neural Operators (FNO) to learn the elastic wave equation from a synthetic training data set. FNO is actually trying to find the manifold for elastic wave propagation. On that manifold, the wave fields are represented with much lower dimensions, and the calculations for wave propagation are simpler compared with the original high dimension. The FNO combines the linear transform, the Fourier transform, and the non-linear local activation, giving the network the power to map from the functional parametric dependence to the wave fields solution. The well-trained Fourier Neural Operator can generate elastic wave fields with good accuracy, and the computational costs for generating the fields used by FNO is about a hundred to a thousand times faster on GPU.

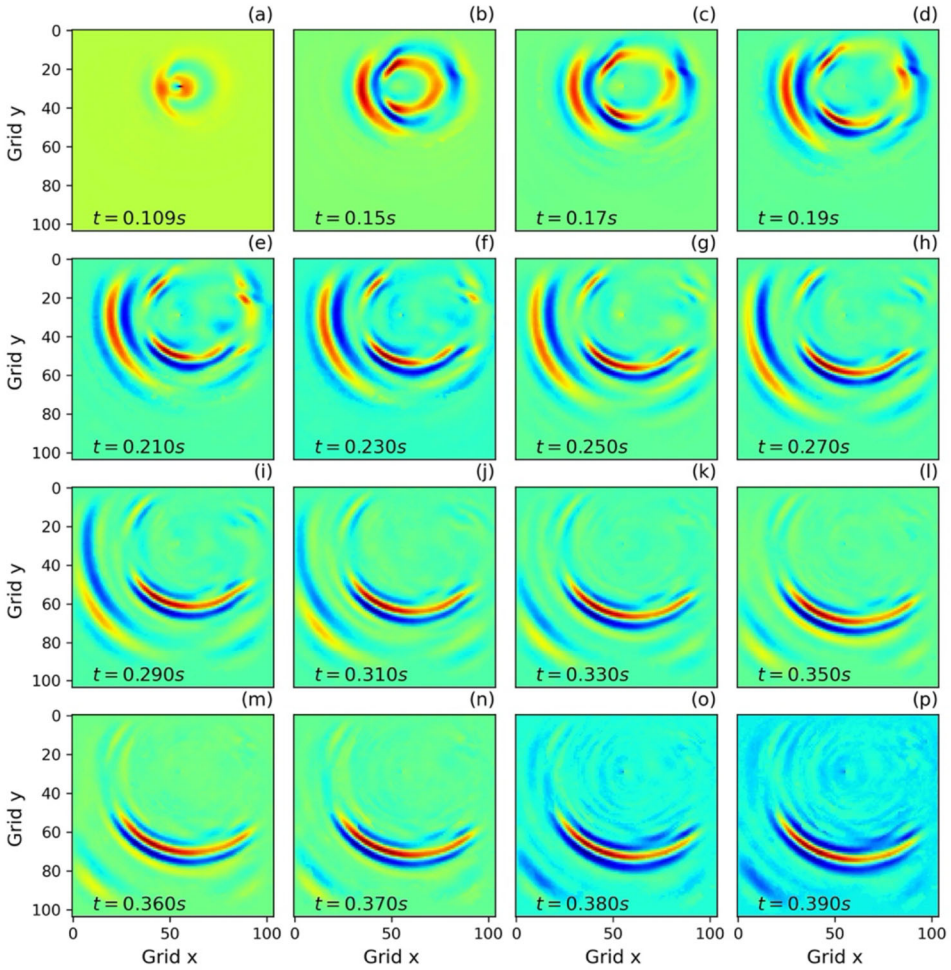

FIG. 1. Nine snap shots of the x component of the wavefields generated with the FNO. With dimension projection width 60 and 33 Fourier models.

The objective functions and adjoint sources behavior for elasticfull waveform inversion

Tianze Zhang and Kristopher Innanen

ABSTRACT

Elastic full-waveform inversion is an ill-posed data-fitting procedure that is sensitive to noise, inaccuracies of the starting model, the definition of multi-parameter classes, and inaccurate modeling of wave fields amplitudes. The objective function measures the difference between the synthetic data and observed data, which plays an essential role in the convergence property of the elastic wave equation. In this study, we investigate the behavior of the *l*", *l*# norm and the correlation-based objective function in FWI and show the sensitivity of these objective functions with respect to VP, VS, and density. The objective functions show that all three objective functions show strong non-linearity with the VS parameter, which means the inversion is relatively harder to invert compared with the other two parameters since it contains a lot of local minimums. We also developed an objective function based on the multi-scale Z transform. The multi-scale Z transform objective function could release the non-linearity of the objective function since the low frequency information of the objective function is first extracted. Thus, the adjoint source contains low frequency information, which helps to build the larger-scale information of the velocity model.

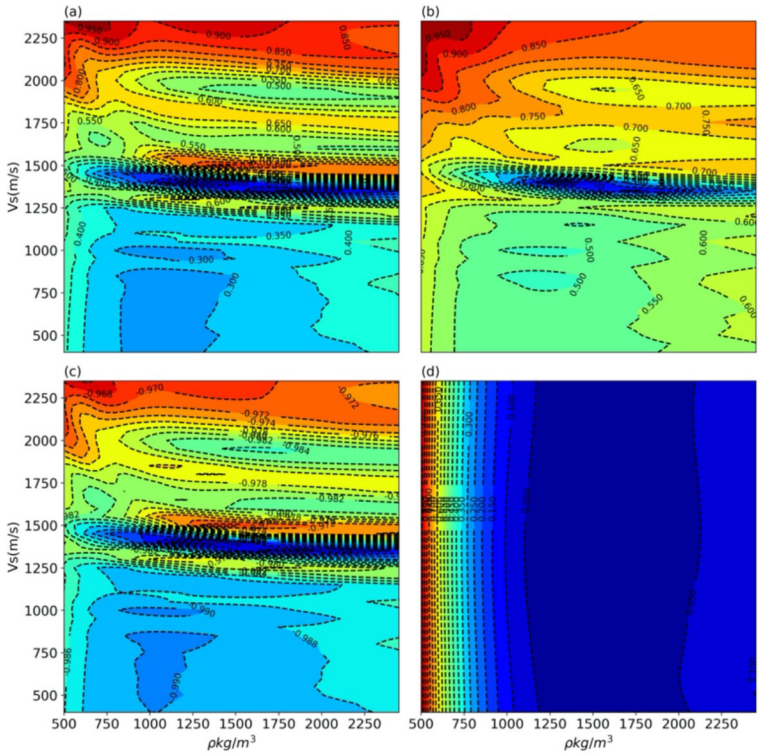

FIG. 1. Contour plot of the different objective functions with the variation of the VS and ρ . (a) l_2 norm. (b) l_1 Norm. (c) Zero lag correlation objective function. (d) Multi-scale Z transform.

Application of GPU processing for acceleration of the non-uniform discrete Fourier transform

Kai Zhuang and Daniel Trad

ABSTRACT

We implemented a non-uniform discrete Fourier transform(NUDFT) algorithm in C++ on both CPU and GPU. In this paper, we explore the advantages and challenges of the implementation of the CUDA API on the non-uniform discrete Fourier transform. The implementation of CUDA is interesting in this application because the non-uniform transform is very time-consuming on the CPU due to O(n2) complexity and the high amounts of memory operations that are performed due to the non-uniform natures of the transform. We implement the NUDFT in CUDA to see if the superior multi-threading performance of GPUs can offset the losses due to memory operations, to make NUDFT and in extension interpolation via NUDFT a computationally viable alternative. The introduction of GPU processing allows us to implement operators that are generally too expensive to implement on the CPU even through the use of large clusters. In our comparison, we show that when properly implemented, the discrete Fourier transform on GPU can perform much faster than its CPU counterpart. The difference results in computational time which may make it economically more acceptable for use in industry. This speedup may allow for the implementation of the DFT in programs such as 5D interpolation or curvelet transforms without the need for local binning. We also note that due to unexpected memory operations the prepackaged Thrust toolkit matrix operators cause significant slowdowns to the calculations.

Processor (API)	Time for 25 shots (s)
i5 8600 6-core (openMP)	1.5996
i7 8750H 6-core (openMP)	1.752
TR 3960x 24-core (openMP)	0.8539
GTX 1080 (CUDA)	0.0447
GTX 1080 (CUDA THRUST)	276.43
RTX 2060 MAX-Q (CUDA)	0.0563
RTX 2060 MAX-Q (CUDA THRUST)	304.43
RTX 3080 (CUDA)	0.0379

Table 1. Table of average runtimes for DFT implementation.